Acoustics of humid porous media: Effects of precondensation and molecular diffusion on their effective properties

Cécile Guianvarc'h,[1] Mohammad Morovati Sharifabadi,[1] Bruno Morvan,[1] Gaëlle Poignand,[2] Fabien Chevillotte,[3] Camille Perrot,[4] and Michel Bruneau[5]

[1)] *Université Le Havre Normandie, CNRS, Normandie Univ, LOMC UMR 6294, 76600 Le Havre, France*

[2)] *Laboratoire d'Acoustique de l'Université du Mans (LAUM), UMR 6613, Institut d'Acoustique - Graduate School (IA-GS), CNRS, Le Mans Université, 72085 Le Mans Cedex 9, France*

[3)] *Matelys – Research Lab, 7 rue des Maraîchers, Bât. B, 69120 Vaulx-en-Velin, France*

[4)] *Univ Gustave Eiffel, Univ Paris Est Créteil, CNRS, UMR 8208, MSME, F-77454 Marne-la-Vallée, France*

[5)] *Laboratoire d'Acoustique de l'Université du Mans (LAUM), UMR 6613, Institut d'Acoustique - Graduate School (IA-GS), CNRS, Le Mans Université, France*

(*Electronic mail: cecile.guianvarch@univ-lehavre.fr)

(Dated: 26 November 2025)

A theoretical approach is developed to describe the acoustic behavior of humid air-saturated porous media. Humid air is here considered as a binary mixture of dry air and water vapor, in which water vapor is likely to precondense (i.e. to be adsorbed) on a solid wall. The formulation of the acoustic problem includes the Navier-Stokes, mass conservation, heat diffusion, and mutual diffusion of water vapor in air equations. The boundary conditions account for the velocities continuity and the mass and heat fluxes conservation at the gas-liquid-solid interfaces. Indeed, precondensed water vapor forms a thin liquid film on the walls that undergoes thickness variations, resulting in non-zero vibration velocity at the liquid-gas interface. This film also acts as a mass and heat source. Its overall behavior is determined by the expression of its thermodynamic equilibrium with water vapor. The problem is analytically solved for straight pores having a constant cross-section shape. The results obtained highlight the specific contributions of precondensation to the dynamic behavior of simple porous structures. These contributions, which are significant under extreme environmental conditions, essentially result in increasing the low-frequency limit of the normalized dynamic compressibility. Based on this analysis, a simple generalization to porous media is also proposed.

NOMENCLATURE

$\alpha(\omega)$	dynamic tortuosity, see eq. (52)
α_P, α_T	baro and thermodiffusion coefficients, see eq. (4)
$\beta(\omega)$	normalized dynamic compressibility, see eq. (31)
Δ	laplacian operator
$\delta, \delta', \delta''$	thicknesses of viscous, thermal and concentration boundary layers
$\dot{d}$	liquid film thickness variation velocity, see eq. (17a)
ϵ	$\frac{\gamma-1}{\gamma} k_T \alpha_T$, see eq. (22)
η	dynamic shear viscosity
Γ	expresses the contrast between humid air and solid wall thermal properties, see eq. (A7)
γ	heat capacity ratio
κ	thermal conductivity of the mixture
κ_ℓ	thermal conductivity of the liquid water
κ_s	thermal conductivity of the solid wall
Λ	viscous characteristic length
Λ'	thermal characteristic length
μ_c	chemical potential by unit mass of water adsorbed by the solid wall, see eq. (39a)
ν	kinematic viscosity, see eq. (3)
ν'	thermal diffusivity, see eq. (3)
ν'_m	modified thermal diffusivity, see eq. (21)
Ω	homogenisation volume
ω	angular frequency
Ω_f	fluid volume
ϕ	porosity, see eq. (46)
$\psi_X(z_3)$	functions describing the temperature, concentration or particle velocity field normal to the boundary
$\rho(\omega)$	effective density, see eq. (27)
ρ_0	static mass density of humid air

ρ_ℓ	static mass density of liquid water
ρ_s	mass density of the solid wall
τ	temperature variation of humid air
τ_ℓ	temperature variation in the liquid film, see eq. (A1)
Θ	$\sqrt{\frac{\rho_s C_s \kappa_s}{\rho_\ell C_\ell \kappa_\ell}}$, see eq. (A4)
φ, φ_0	total and static relative humidity, see eq. (1)
$\mathbf{i}$	concentration flux density of dry air, see eq. (5)
$\boldsymbol{\nabla}_{12}$	two-dimensional gradient along z_1, z_2
$\mathbf{q}$	heat flux in humid air, see eq. (12)
$\mathbf{v}$	particle velocity of humid air
ξ	related to the displacement of the liquid-gas interface, see eq. (18b)
c_0	adiabatic speed of sound in humid air
C_ℓ	heat capacity of liquid water
C_P, C_V	isobaric and isochoric specific heat capacities
C_s	heat capacity of the solid wall
D	molecular diffusion coefficient
d, d_0	total and static thickness of the condensation liquid film
D_m	modified molecular diffusion coefficient, see eq. (21)
$f_v(P,T)$	enhancement factor, see eq. (1)
F_X	mean value over a cross-section of function $\psi_X(z_3)$
h_L	proportional to L, see eq. (18d)
h_s	see eq. (17b)
$J_n(r)$	nth order Bessel function of first kind
$k'(\omega)$	dynamic thermal permeability
$K(\omega)$	effective bulk modulus, see eq. (30)
$k(\omega)$	dynamic permeability, see eq. (50)
k_0	static viscous permeability, see eq. (48)
k'_0	static thermal permeability
k_P, k_T	baro and thermodiffusion ratios of dry air inside water vapor
L	latent heat of water vapor per unit mass of liquid
M	molar mass of humid air, see eq. (2)
M_a, M_v	molar masses of dry air and water vapor
p	pressure variation of humid air
P, P_0	total and static pressures
$P_s(T)$	water saturation vapor pressure
P_v	partial pressure of water vapor in humid air, see eq. (1)
P_{sv0}	$f_v(P_0,T_0)P_s(T_0)$, see eq. (17a)
R	radius of a cylindrical pore
S	cross-section of the waveguide
S_e	exchange surface of the waveguide
T, T_0	total and static temperatures
V	volume of the waveguide
V_t	total volume of porous material
w	mass fraction variation of dry air
W, W_0	total and static mass fractions of dry air
x_a, x_v	mole fractions of dry air and water vapor
z_1, z_2, z_3	space coordinates, see Fig. 1

I. INTRODUCTION

What are the effects of moisture content on the acoustic properties of porous media? How do macroscopic transport properties depend on the relative humidity of air? These are among the key questions that have driven fundamental studies on the dynamic and thermodynamic behavior of moist air in porous materials such as sandy soils, wet stacks, or architected media. These issues can be addressed in several ways. Perhaps the most direct approach consists of performing a series of laboratory measurements on samples of various types and moisture contents to determine the macroscopic parameters of equivalent fluid models; they may, however, require great expense, and are usually limited to sample types with very specific morphologies[1–5]. Alternatively, in the pursuit of a theoretical understanding, one may seek to elucidate the mathematical or physical foundations of the Darcy-scale equations for saturated porous media involving two distinct fluids, though this approach neglects possible molecular diffusion processes between the liquid and gas phases[6]. Finally, first-principles studies have been carried out to describe successive evaporation and condensation phenomena in the presence of an acoustic wave, but these have yet to be experimentally validated[7–12]. Each of these approaches, in fact, presents its own strengths and weaknesses.

When examining previous contributions in the field of thermoacoustics, several studies can be found on acoustic propagation in porous media composed of straight pores. These works aim to characterize the effects of water — liquid and vapor with possible phase change — on the performance of thermoacoustic machines (e.g., efficiency, instability, onset temperature). Both modeling and experimental results indicate that the presence of water helps improve the performance of these machines[8,13–17].

A significant portion of research on architected or porous media has also been encompassed within the broader field of acoustic metamaterials — engineered structures whose effective acoustic properties differ significantly from those of conventional media, thereby providing a powerful means to control elastic wave propagation (e.g., filtering, cloaking, guiding, focusing)[18]. The concept of acoustic tunability has rapidly emerged as a major research focus, and several strategies have been developed to modulate the effective acoustic response of architected structures[19–23]. Among these approaches, some exploit water as an external control parameter, playing a role analogous to that of a tunable element in humidity-sensitive acoustic systems. Studying the effects of humidity on the acoustic properties of architected materials could therefore open new possibilities for the design of smart materials.

One challenge in studying the effects of humidity on the acoustic properties of porous media and metamaterials arises from the ambiguity of the term "humidity", which may refer either to the moisture content of a material—characterizing the amount of liquid water it contains—or to the relative humidity of the air occupying its pores. One of the purposes of this paper is to clarify this distinction. The moisture content of a material can clog pores and modify their mechanical and thermal properties (e.g., density, heat capacity, thermal conductivity). In contrast, the relative humidity of air, that depends on both the water molar fraction and the temperature, is expected to primarily influence the physical properties of the air saturating the pores[24,25], without fundamentally altering the well-established viscous and thermal dissipative mechanisms within them[26–28].

Finally, it should be noted that previous studies on acoustic methods for gas metrology have reported a significant coupling between the acoustic field in vapor-filled closed cavities and a phenomenon known as "precondensation" of vapor on solid surfaces[29,30]. The precondensed liquid film is described as an equilibrium phenomenon caused by different intermolecular potentials between vapor and wall-surface molecules. This phenomenon is equivalent to adsorption[31], that is, the adhesion of gas molecules to a solid surface driven by surface forces. Consequently, a liquid layer may be formed on a solid wall even though the saturation point of the vapor is not reached.

Following this overview of the various possible mechanisms, the relative humidity of air can have several distinct effects on the acoustic properties of a porous material saturated with humid air. These effects may arise from *(i)* an alteration of the physical properties of humid air, *(ii)* the presence of a liquid film coating the pore walls, which can reduce the effective pore size or even eliminate an entire porosity scale, or *(iii)* cyclic phase changes of the liquid layer, which may act both as a vibrating surface and as sources of mass and heat.

In the present paper, our aim is therefore to provide a comprehensive analytical description of acoustic propagation in humid air. By doing so, we hope to provide a fundamental basis for investigating the acoustic behavior of porous materials within the framework of equivalent fluid models, and more generally, to highlight the properties of porous materials over a broad range of environmental conditions.

In Section II, we introduce a formulation of the acoustic problem in humid air, treated as a binary mixture of dry air and water vapor. This formulation builds upon those presented in previous works[9,32], with simplifying assumptions adapted to the study of acoustic propagation in porous media saturated with humid air. It should be emphasized that the main differences between this work and previous studies on similar phenomena[8,12] lie in the working hypotheses underlying the formulation of the acoustic problem within the propagation domain (these discrepancies are discussed as the main hypotheses are introduced below). Analytical solutions to this problem are then developed in Section III for a straight waveguide (cylindrical tube or rectangular slit), allowing the effective dynamic density and compressibility of the propagation medium to be expressed explicitly. Section IV presents theoretical results obtained for a straight cylindrical pore under atmospheric and extreme environmental conditions, in order to highlight the physical mechanisms that primarily affect the effective properties of humid air in the waveguide and to identify relevant simplifications. The results also reveal the limitations of several commonly accepted simplifying assumptions, which will need to be revisited in future work. Finally, Section V extends the proposed formalism to porous media, whose intrinsic properties are determined from asymptotic developments.

II. PROBLEM FORMULATION AND SOLUTIONS CLOSE TO BOUNDARIES

Before expressing the acoustic problem, we first provide in section II A clarifications about relative humidity of air. Then we detail in paragraph II B the variables chosen here to describe the dynamic and thermodynamic behavior of moist air (considered here as a binary gas mixture) as well as the parameters specifying the state of the mixture, as some of them are not usual in acoustics.

We thus express the acoustic problem by *(i)* linear equations simplified for gas-vapor mixture saturated in closed spaces, in which dissipation in the bulk of the fluid

is neglected (§ II C), *(ii)* a complete set of boundary conditions that account for evaporation and condensation processes at the gas-liquid interface (§ II D).

A. Relative humidity of air

Relative humidity, generally expressed as a percentage, is a measure of the closeness of the partial pressure of water vapor in the air $P_{v0} = x_v P_0$ to the water saturation vapor pressure $P_s(T_0)$. This quantity is defined as follows:

$$\varphi_0 = \frac{P_{v0}}{f_v(P_0, T_0) P_s(T_0)} = \frac{x_v P_0}{f_v(P_0, T_0) P_s(T_0)}, \quad (1)$$

where the value of ambient temperature T_0 lies between those of the triple and critical points of water (i.e. $273.16\ K < T_0 < 647.096\ K$) and where the enhancement factor $f_v(P_0, T_0)$ expresses the fact that the dilution of water vapor in air slightly alters the effective value of water saturation vapor pressure. Therefore, the relative humidity of air is indicative not only of the water vapor amount in the air, but also of its proximity to the saturation point. As previously stated, precondensation (or adsorption) occurs even at vapor pressures below the saturation vapor pressure, and increases as the vapor approaches the saturation point. This process is thus directly related to the proximity of the vapor under study to its saturation point; that is to say, considering the water vapor in the air, to the relative humidity of air.

B. Parameters and variables describing the state and behavior of humid air

We consider humid air as a binary gas mixture or dry air and water vapor, the water vapor being sufficiently close to saturation to condensate on a solid wall due to molecular interactions between the vapor and the solid interface[9,32].

The parameters specifying the state of humid air are the static pressure P_0, temperature T_0 and mass fraction of dry air W_0 (or the static mass fraction of water vapor $1 - W_0$), and the density ρ_0.

The nature of this binary gas mixture is determined by the molar fractions of dry air x_a and water vapor $x_v = 1 - x_a$, the molar mass of humid air being thus written as

$$M = x_a M_a + x_v M_v = M_a + (M_v - M_a) x_v, \quad (2)$$

M_a and M_v being the molar masses of dry air and water vapor respectively.

Several physical properties of humid air are subsequently impacted by its nature and state, namely the heat capacities at constant pressure and constant volume per unit of mass C_P and C_V respectively, the heat capacity ratio $\gamma = C_P/C_V$, the adiabatic speed of sound c_0, the dynamic shear viscosity η and the thermal conductivity κ of the mixture. The kinematic viscosity and the thermal diffusivity are thus given by

$$\nu = \frac{\eta}{\rho_0}, \quad \text{and} \quad \nu' = \frac{\kappa}{\rho_0 C_P}. \quad (3)$$

Since we consider humid air as a binary gas mixture, we must add to the previous transport properties the molecular diffusion coefficient D, the baro and thermodiffusion ratios k_P and k_T respectively[33]. These three quantities describe the diffusion of each component of a binary gas mixture into the other under the effects of mass diffusion, pressure variations (barodiffusion) and temperature variations (thermodiffusion). It is worth noting that D can be expressed as an inverse function of static pressure P_0[34], implying naturally that mass transfers by molecular diffusion processes are favoured at low static pressures. Moreover, k_P and k_T are equal to zero in a pure gas and maximum for a 50%-50% binary gas mixture because they are both proportional to $x_a x_v$,. We can also define the baro and thermodiffusion coefficients as

$$\alpha_P = \frac{k_P}{x_a x_v} = \frac{M_v - M_a}{M} \quad \text{and} \quad \alpha_T = \frac{k_T}{x_a x_v}. \quad (4)$$

Finally, we describe the dynamic and thermodynamic behavior of humid air submitted to an acoustic movement with the following variables: the pressure variation p, the particle velocity $\mathbf{v}$, the temperature variation τ of the dry air - water vapor mixture and the mass fraction variation of dry air w (i.e. $1 - w$ for water vapor).

The molecular diffusion process also involves the concentration flux density of dry air, which is given by[33]

$$\mathbf{i} = -\rho_0 D \left[\boldsymbol{\nabla} w + \frac{M_a M_v}{M^2} \frac{k_P}{P_0} \boldsymbol{\nabla} p + \frac{M_a M_v}{M^2} \frac{k_T}{T_0} \boldsymbol{\nabla} \tau \right]. \quad (5)$$

This expression highlights the molecular diffusion process being actually driven by the three diffusion processes described above.

Even though the concentration flux density $\mathbf{i}$ is fundamental to describe the molecular diffusion process, in particular in confined spaces, we chose to express the acoustic problem for the variables $\mathbf{v}$, p, τ and w in particular for the simplicity of working with a scalar quantity instead of a vectorial one. Of course, the acoustic problem can be expressed for $\mathbf{i}$ instead of w as well.

C. Linear equations of acoustics close to boundaries

The linear equations governing acoustic fields in humid air, considered as a gas-vapor mixture, recalled in this section, all rely on the following ones[9,32,33]:

- the Navier-Stokes equation for the mixture,
- the mass conservation equation for the mixture and for one component of the mixture,

- thermodynamic expressions for entropy and density variations,
- the Fourier's equation,
- the expression of the concentration flux density (5).

These equations are linearized and expressed for a harmonic movement of angular frequency ω ($e^{j\omega t}$ convention). Also note that, in the modelling developed here, with the inwardly directed coordinate normal to the wall z_3 (Fig. 1), we consider $\sqrt{-j} = (1-j)/\sqrt{2}$.

The general formulation proposed previously by Guianvarc'h and Bruneau[32] for the acoustic problem far from and close to boundaries is simplified here for describing the acoustic behaviour of humid air in confined spaces as represented in Figure 1. The terms expressing the dissipation in the bulk of the fluid are thus neglected.

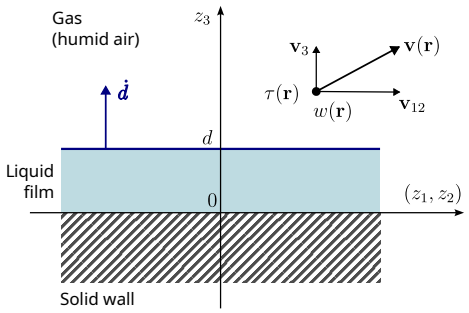

FIG. 1. Particle velocity, temperature and air concentration variation fields close to a boundary coated with a condensation liquid film.

The tangential and normal particle velocities, $\mathbf{v}_{12}$ and v_3, as well as the temperature and concentration variations, τ and w respectively are governed by the following set of equations:

$$\frac{\partial}{\partial z_3} v_3 + \boldsymbol{\nabla}_{12} \cdot \mathbf{v}_{12} = -j\omega \left(\frac{p}{P_0} - \frac{\tau}{T_0} - \alpha_P \frac{M^2}{M_a M_v} w \right) , \tag{6a}$$

$$j\omega \rho_0 \mathbf{v}_{12} = -\boldsymbol{\nabla}_{12} p + \eta \frac{\partial^2}{\partial z_3^2} \mathbf{v}_{12} , \tag{6b}$$

$$j\omega \rho_0 C_P \tau = \kappa \Delta \tau + j\omega \left(p + P_0 \alpha_T \frac{M^2}{M_a M_v} w \right) , \tag{6c}$$

$$j\omega w = D\Delta w + D \frac{M_a M_v}{M^2} \left(\frac{k_P}{P_0} \Delta p + \frac{k_T}{T_0} \Delta \tau \right) , \tag{6d}$$

where $\mathbf{v}_{12}$ and $\boldsymbol{\nabla}_{12}$ are respectively the two-dimensional particle velocity and gradient along (z_1, z_2), where v_3 is the component of the particle velocity normal to the wall (z_3 coordinate) and Δ is the laplacian operator. In equations (6a-d), the dissipation processes in the bulk are neglected since we assume that the predominant dissipative phenomena are those occurring throughout the viscous, thermal and concentration boundary layers, whose respective thicknesses are given by

$$\delta = \sqrt{\frac{2\nu}{\omega}}, \quad \delta' = \sqrt{\frac{2\nu'}{\omega}}, \quad \delta'' = \sqrt{\frac{2D}{\omega}}. \tag{7}$$

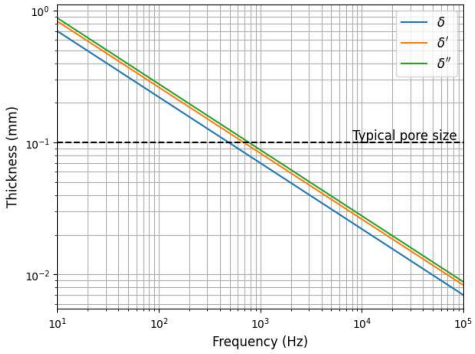

FIG. 2. Thicknesses of the viscous, thermal and concentration boundary layers as function of the frequency with an example of typical pore size in acoustic materials

.

As illustrated in Figure 2, within the audio frequency range, the thickness of the viscous, thermal, and concentration boundary layers remains comparable to the typical pore sizes of microstructured materials. Therefore, in such materials, main dissipative phenomena are confined to the boundary layers since bulk dissipation acts as a higher-order term[9,32].

In several previous theoretical approaches[8,12,35], molecular diffusion due to pressure and temperature variation were not considered. As a result, the baro and thermodiffusion coefficients, α_P and α_T, respectively, were neglected in these works, which is a reasonable assumption given the order of magnitude of these coefficients (see Table I). However, since we intend to provide here analytical solutions to the acoustic problem in simple geometries (straight cylindrical or rectangular pores), we can consider all the molecular diffusion phenomena involved, and we shall keep all the related terms to evaluate their relative contributions *a posteriori*.

D. Boundary conditions

Since the partial pressure $P_v = x_v P$ of water vapor in air (at temperature T) is close to, but less than, the water saturation vapor pressure $P_s(T)$, condensation is likely to occur on a solid interface, which is thus coated

by a liquid film whose thickness increases as the pressure P_v approaches P_s. As acoustic movement involves both pressure and temperature variations, it results in successive evaporation and condensation phenomena on the wall during an acoustic cycle. Consequently, under the effect of an acoustic field, the condensation film undergoes thickness variations (vibratory velocity linked to phase changes), but it also generates *(i)* molecular diffusion of water vapor from the boundary to the propagation domain, and *(ii)* heat transfers that involve latent heat of water vapor. Furthermore, considering moist air as a binary gas mixture of dry air and water vapor, pressure and temperature variations are also coupled with local water vapor (or dry air) concentration variations[32]. The general solutions of eq. (6a-d) are subjected to the following boundary conditions at the liquid-gas interface $z_3 = d$ (see Fig. 1), that involve all these physical phenomena. These boundary conditions are essentially those previously proposed by Guianvarc'h et al[9]. Some of them are detailed in Appendix A and B.

1. Particle velocity

The tangential components $\mathbf{v}_{12}$ of the particle velocity of the mixture vanish (non-slip condition):

$$\mathbf{v}_{12}(d) = \mathbf{0}\,. \tag{8}$$

The thickness d of the liquid film is subjected to oscillations around the static value d_0 as water vapor successively evaporates and condensates during an acoustic cycle, described by its vibration velocity $\dot{d} = \partial d/\partial t$. At the liquid-gas interface $z_3 = d$, the normal component of air particle velocity is thus equal to the vibration velocity $\dot{d}$, that leads to the following expression[9]:

$$\left.\frac{\partial p}{\partial z_3}\right|_d \approx j\omega\rho_\ell \dot{d}\,, \tag{9}$$

at the lowest order of approximation and under the reasonable assumption that mass density of liquid water ρ_ℓ is much greater than that of dry air. This result shows that the spatial variation of the acoustic pressure in the direction normal to the wall is non zero, due to the thickness variations of the liquid film. The terms expressing the effects of molecular diffusion due to pressure variations (barodiffusion) are thus significant close to the boundaries and should not be neglected here.

2. Concentration flux density

The component normal to the wall i_3 of the concentration flux density of dry air is related to the vibration velocity of the liquid film $\dot{d}$ as follows[9]:

$$i_3(d) = x_a \frac{M_a}{M}\rho_\ell \dot{d}\,. \tag{10}$$

According to equation (5), $\mathbf{i}$ is also a function of the pressure, temperature and concentration variations gradients, that leads, making use of eq. (9), to

$$\left(1 + j\omega D\rho_0 x_v \frac{M_v}{M}\frac{\alpha_P}{P_0}\right) x_a \frac{M_a}{M}\rho_\ell \dot{d} = - \rho_0 D\left[\frac{\partial w}{\partial z_3} + \frac{M_a M_v}{M^2}\frac{k_T}{T_0}\frac{\partial \tau}{\partial z_3}\right]_d .$$

In the left hand side in this relationship, the second term in the parenthesis is very small with respect to 1 in the frequency range of interest (see orders of magnitude in Table I), we thus neglect it at the lowest order of approximation[9,32]. That leads finally to the following boundary condition

$$x_a \frac{M_a}{M}\rho_\ell \dot{d} \approx -\rho_0 D\left[\frac{\partial w}{\partial z_3} + \frac{M_a M_v}{M^2}\frac{k_T}{T_0}\frac{\partial \tau}{\partial z_3}\right]_d . \tag{11}$$

3. Heat flux

The heat flux $\mathbf{q}$ in humid air involves the temperature gradient as well as the concentration flux density $\mathbf{i}$[32,33]

$$\mathbf{q} = \alpha_T \frac{P_0}{\rho_0}\frac{M^2}{M_a M_v}\mathbf{i} - \kappa\boldsymbol{\nabla}\tau. \tag{12}$$

The continuity of heat flux normal to the wall at the liquid-gas interface $z_3 = d$ involves also a slight temperature variation on the liquid boundary due to the latent heat of water vapor per unit mass of liquid L[9,12,29], that leads to, accounting for eq. (10),

$$\begin{aligned} q_3(d) &= \frac{k_T}{x_v}\frac{P_0}{\rho_0}\frac{M}{M_v}\rho_\ell \dot{d} - \kappa\left.\frac{\partial \tau}{\partial z_3}\right|_d \\ &= q_\ell(d) + \rho_\ell L\dot{d}, \end{aligned} \tag{13}$$

$q_\ell(z_3)$ being the heat flux in the liquid film, normal to the wall, whose expression is detailed in appendix A.

Given this and expression (A6) established for $q_\ell(d)$ in appendix A, the conservation of heat flux and the temperature continuity at the solid-liquid ($z_3 = 0$) and liquid-gas ($z_3 = d$) interfaces lead to the following relationship

$$\Gamma\rho_\ell\left(L - \frac{k_T}{x_v}\frac{M}{M_v}\frac{P_0}{\rho_0}\right)\dot{d} = j\sqrt{-j\omega\rho_0 C_P\kappa}\,\tau(d) - \Gamma\kappa\left.\frac{\partial \tau}{\partial z_3}\right|_d , \tag{14}$$

where the expressions of Γ given in appendix A (see eq. A7) involves a parameter Θ that is given by eq. (A4).

We must draw the attention to the interpretation of the factors Γ and Θ that makes them relevant parameters to the description of the phenomena inside the boundary layers, because they both involve the ratio of contrasted

thermal properties, respectively between the gas and the solid wall through the liquid film of thickness d (Γ) and between the solid and the liquid (Θ). Moreover, it is worth noting that, when the thickness of the liquid film d vanishes, the parameter Γ involves only the contrast of thermal properties between the gas and the solid as shown at the end of appendix A.

This boundary condition is comprehensive, as it accounts for heat transfers at the solid-liquid and liquid-gas interfaces, as well as mass transfers by thermodiffusion process (term involving k_T). However, its complexity appeals simplifications by considering the orders of magnitude of Γ and Θ in humid air for several possible materials.

For instance, with materials such as nichrome or aluminium (used in thermoacoustic engines), Γ is of the order of a few 10^{-4} for the real part and at most a few 10^{-6} for the imaginary part. This factor Γ depends weakly on heat transfers within the liquid film, insofar as Θ is large compared to $|\tan k_\ell d|$, i.e. the liquid layer is thinner than the thermal penetration depth in water. This condition is met under the reasonable assumption that the thickness of the film remains on the order of a few tens of nanometres, as outlined in section IV.

However, for thermal insulation materials such as cork, Θ is much smaller, and Γ can reach values on the order of a few 0.01 and 0.001 for the real and imaginary parts respectively, the thickness of the liquid film coating the wall having a significant effect here. However, note that the thermal properties of these materials are related to their microporous structure. The presence of adsorbed liquid water within this microstructure is therefore likely to have a significant impact on the overall thermal properties of the material, and the estimates provided here should be substantially refined.

In many practical applications, we can reasonably assume that Γ is nearly equal to zero. This amounts to neglecting heat transfers associated with evaporation and condensation processes and leads to isothermal boundary conditions at the liquid-gas interface ($\tau(d) = 0$). For the sake of generality, we keep the thermal boundary condition (14) in the following discussion, but at each step of the analytical development, we also consider the specific case $\Gamma = 0$.

Finally, should the latent heat L be sufficiently high, the term $\Gamma\rho_\ell L$ in the left-hand side of eq. (14) could also be significant. This fully justifies retaining all terms related to heat transfers through the gas-liquid-solid interfaces of this boundary condition, as done in other previous works[8,12].

4. Liquid film coating the solid wall

The time derivative $\dot{d}$ of the liquid film thickness d, which is involved in several boundary conditions, should be expressed here as a function of the variables describing the acoustic behavior of humid air. As outlined in the literature[29,31,36], precondensation and adsorption phenomena heavily depend on the ratio of the vapor pressure P_v to the saturation vapor pressure P_{sv}, i.e. on the relative humidity φ. We also note a weak influence of the ambient temperature T. Finally, for the purpose of this study, we assume that the thickness of the precondensed liquid film is an increasing function of relative humidity $d(\varphi)$, with

$$\varphi = \frac{P_v}{f_v(P,T)P_s(T)} \quad \text{and} \quad P_v = \frac{M_a(1-W)P}{M_a + (M_v - M_a)W}. \tag{15}$$

An example of theoretical expression available in the literature for the function $d(\varphi)$ is detailed in section IV A with a discussion on its validity, but the following formulation applies on other expressions (theoretical or empirical) as well. Whatever the way we chose to express $d(\varphi)$, it has to be a function of total pressure, temperature and dry air mass concentration, P, T, W, respectively. This leads thus to the following differential linear expression for the velocity $\dot{d}$ of the liquid-gas mixture interface ($z_3 = d$):

$$\dot{d} = \frac{\mathrm{d}d}{\mathrm{d}\varphi}\left[\left(\frac{\partial\varphi}{\partial P}\right)_{T_0,W_0}\frac{\partial p}{\partial t} + \left(\frac{\partial\varphi}{\partial T}\right)_{P_0,W_0}\frac{\partial\tau}{\partial t} + \left(\frac{\partial\varphi}{\partial W}\right)_{T_0,P_0}\frac{\partial w}{\partial t}\right]. \tag{16}$$

The calculation of the partial derivatives involved in the above expression is detailed in Appendix B. Finally, we define $P_{sv0} = f_v(P_0,T_0)P_s(T_0)$ such that we can write the thickness variation velocity $\dot{d}$ as follows, for harmonic motion,

$$\dot{d} \approx j\omega\frac{\mathrm{d}d}{\mathrm{d}\varphi}\frac{P_0}{P_{sv}}\left[x_v\frac{p(d)}{P_0} - x_v h_s\frac{\tau(d)}{T_0} - \frac{M^2}{M_a M_v}w(d)\right], \tag{17a}$$

where

$$h_s = \frac{T_0}{P_{sv}}\left(\frac{\partial P_{sv0}}{\partial T}\right)_{P_0,T_0}. \tag{17b}$$

This model is fundamentally different from the approach proposed by Boutin and Venegas[12], who also introduce a parameter similar to $\dot{d}$ describing the liquid film coating the wall as a water mass variation on the wall. This parameter has not to be expressed in their formalism, as it is removed by using eq. (11) into (13). The thermodynamic equilibrium of water (liquid and vapor) on the wall is thus expressed throughout the Clapeyron relation. The use of this relation would imply that the partial pressure of water vapor in air P_v is always equal to the water saturation vapor pressure $P_s(T)$, and the relative humidity is thus close to 100%.

5. Coupled boundary conditions on temperature and concentration variations

Finally, we make use of eq. (17a) into eqs. (11) and (14) in order to remove $\dot{d}$. This leads to the following boundary conditions on both τ and w:

$$\frac{k_T}{T_0}\frac{\partial \tau}{\partial z_3}\bigg|_d + \frac{M^2}{M_a M_v}\frac{\partial w}{\partial z_3}\bigg|_d = -\frac{j\omega}{D}x_a\xi\left[x_v\frac{p(d)}{P_0} - x_v h_s\frac{\tau(d)}{T_0} - \frac{M^2}{M_a M_v}w(d)\right], \quad (18a)$$

where

$$\xi = \frac{\mathrm{d}d}{\mathrm{d}\varphi}\frac{M}{M_v}\frac{\rho_\ell}{\rho_0}\frac{P_0}{P_{sv0}} \quad (18b)$$

is related to the liquid film thickness variation, and

$$\Gamma\left(h_L - \frac{k_T}{x_v}\right)\frac{P_0}{\rho_0 C_p}\frac{j\omega}{\nu'}\xi\left[x_v\frac{p(d)}{P_0} - x_v h_s\frac{\tau(d)}{T_0} - \frac{M^2}{M_a M_v}w(d)\right] = j\sqrt{\frac{-j\omega}{\nu'}}\tau(d) - \Gamma\frac{\partial \tau}{\partial z_3}\bigg|_d \quad (18c)$$

with

$$h_L = \frac{\rho_0 L}{P_0}\frac{M_v}{M}. \quad (18d)$$

Actually, the Clausius-Clapeyron relation would allow us to state that $h_s = h_L$ in an ideal gas. However, humid air is a real gas in which the water saturation vapor pressure is slightly modified by the presence of dry air in the gas mixture. Furthermore, these terms h_s and h_L do not formally have the same origin, and we express them separately herein.

When we can consider isothermal boundary conditions at the liquid-gas interface $z_3 = d$ (i.e. $\Gamma = 0$), boundary conditions (18a,c) simply lead to

$$\frac{k_T}{T_0}\frac{\partial \tau}{\partial z_3}\bigg|_d + \frac{M^2}{M_a M_v}\frac{\partial w}{\partial z_3}\bigg|_d = -\frac{j\omega}{D}x_a\xi\left[x_v\frac{p(d)}{P_0} - \frac{M^2}{M_a M_v}w(d)\right], \quad (19a)$$

and

$$\tau(d) = 0 \quad (19b)$$

In any case, all terms factors of ξ in these boundary conditions express the effects of physical phenomena that are coupled to the liquid film thickness variation. Consequently, the boundary conditions of acoustic problems in non-condensing binary gas mixtures[32] are straightforwardly derived from (18a,c) or (19a,b) by setting $\xi = 0$.

E. Solutions

The general solutions of the acoustic problem proposed by Guianvarc'h et al.[9] are recalled below at the lowest order. Note that, for the purpose of the application considered here (wave propagation in porous media), dissipative effects in the bulk are negligible compared to dissipative and reactive phenomena close to the boundary layers.

The solution of equation (6b) for the particle velocity tangent to the wall that accounts for the no-slip condition (8) is written as

$$\mathbf{v}_{12}(z_1, z_2, z_3) \approx -\frac{1}{j\omega\rho_0}\boldsymbol{\nabla}_{12}p(z_1, z_2)[1 - \psi_v(z_3)], \quad (20)$$

where $\psi_v(z_3)$ is the normalized solution of the homogeneous equation associated with (6b).

We remove the concentration variation w in eq. (6c) by making use of eq. (6d), and we obtain a fourth-order equation for τ that involves the thermal diffusivity ν', the molecular diffusion coefficient D, and the "modified" thermal diffusivity and molecular diffusion coefficient ν'_m and D_m respectively, whose definitions[9,32] impose the following relationships:

$$\nu'_m + D_m = \nu' + (1+\epsilon)D \quad \text{and} \quad \nu'_m D_m = \nu' D, \quad (21)$$

with

$$\epsilon = \frac{\gamma - 1}{\gamma}k_T\alpha_T. \quad (22)$$

The solution of this fourth-order equation for τ can be expressed as follows, taking into account the boundary conditions (18a,c):

$$\tau(z_1, z_2, z_3) = \frac{p(z_1, z_2)}{\rho_0 C_P}\left[1 - A\psi_{\tau m}(z_3) - B\psi_{wm}(z_3)\right], \quad (23)$$

where functions $\psi_{\tau m}(z_3)$ and $\psi_{wm}(z_3)$ are the normalized solutions of the homogeneous equation associated with the previous fourth-order equation, the integration constants A and B being given by the boundary conditions (18a,c). The functions $\psi_{\tau m}(z_3)$ and $\psi_{wm}(z_3)$ express the couplings between thermal and molecular diffusion processes in the dry gas–vapor mixture. More specifically, $\psi_{\tau m}(z_3)$ describes thermal diffusion modified by molecular diffusion process, and conversely for $\psi_{wm}(z_3)$. The detailed expressions of these functions are in Appendix C for the case of a cylindrical waveguide and a flat slit.

Consequently, the concentration variation w, solution of eq. (6d) is expressed as follows

$$w(z_1, z_2, z_3) = -\frac{p(z_1, z_2)}{P_0}\frac{x_a x_v}{k_T}\frac{M^2}{M_a M_v}\left[A\left(1 - \frac{\nu'}{\nu'_m}\right)\psi_{\tau m}(z_3) + B\left(1 - \frac{\nu'}{D_m}\right)\psi_{wm}(z_3)\right]. \quad (24)$$

We note that functions $\psi_X(z_3)$ and integration constants A and B directly depend on the geometry of the wall surface and of the propagation domain. The expressions of functions $\psi_X(z_3)$ are left to the Appendix C when considering specific geometries such as a cylindrical tube and a rectangular slit.

III. PROPAGATION IN A WAVEGUIDE

We consider a waveguide of cross-section S, volume V and exchange surface S_e. As shown in Figure 3, the propagation domain is limited by the condensation liquid film coating the walls of the waveguide. In this case, given the symmetry of the problem, the space coordinate z_3 remains oriented inwards and normal to the walls within the propagation domain.

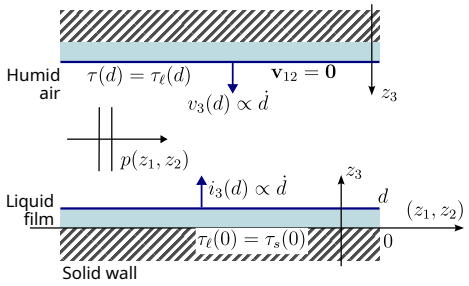

FIG. 3. Acoustic propagation in a waveguide, boundary conditions on the particle velocity, temperature variation and dry air concentration flux density.

If we assume a "quasi-plane" wave propagation in the direction (z_1, z_2), the acoustic propagation in the waveguide is described by *(i)* the pressure variation p, which is supposed to be constant along the z_3 axis, and *(ii)* the mean values over the cross-section S of the variables $\mathbf{v}_{12}$, τ, w, defined as

$$\langle \cdot \rangle = \frac{1}{S} \int_S \cdot \, \mathrm{d}\mathcal{S}. \tag{25}$$

A. Effective density

The mean value of solution (20) for the particle velocity component tangential to the wall takes the well-known following form

$$j\omega\rho(\omega)\langle \mathbf{v}_{12} \rangle = -\boldsymbol{\nabla}_{12} p, \tag{26}$$

in which the effective density of humid air in the pore is given by

$$\rho(\omega) = \frac{\rho_0}{1 - F_\nu}, \tag{27}$$

where $F_\nu = \langle \psi_v \rangle$ involves the kinematic viscosity ν and depends on the shape of the waveguide (see appendices C 1 and C 2).

As expected, the successive evaporation and condensation processes during an acoustic cycle have no effect on the effective density of humid air within a straight pore. However, as outlined in Section II D 4, the static thickness d_0 of the liquid film coating the wall should increase as the partial pressure of water vapor in air, P_{v0}, approaches the saturation pressure P_{sv0}. Consequently, the static thickness of the liquid film slightly decreases the pore size and thus the viscous permeability. As long as d_0 is much smaller than the size of the pores, no significant alteration of the effective density due to water precondensation is expected.

B. Normalized dynamic compressibility

Remembering that the mean value of the normal velocity v_3 over the cross-section S of the waveguide is zero and making use of equation (6a) yields

$$-\boldsymbol{\nabla}_{12} \cdot \langle \mathbf{v}_{12} \rangle = -j\omega \left(\frac{p}{P_0} - \frac{\langle \tau \rangle}{T_0} - \alpha_P \frac{M^2}{M_a M_v} \langle w \rangle \right). \tag{28}$$

We thus make use of expressions (23) and (24) in order to establish the following relationship

$$-\boldsymbol{\nabla}_{12} \cdot \langle \mathbf{v}_{12} \rangle = \frac{j\omega}{K(\omega)} p \tag{29}$$

in which the effective bulk modulus $K(\omega)$ can be written as

$$\frac{1}{K(\omega)} = \frac{\beta(\omega)}{\gamma P_0}, \tag{30}$$

the normalized dynamic compressibility being given by

$$\begin{aligned} \beta(\omega) &= 1 + (\gamma - 1)(A F_{\nu'_m} + B F_{D_m}) \\ &+ \gamma \frac{k_P}{k_T} \left[\left(1 - \frac{\nu'}{\nu'_m} \right) A F_{\nu'_m} + \left(1 - \frac{\nu'}{D_m} \right) B F_{D_m} \right], \end{aligned} \tag{31}$$

where $F_{\nu'_m} = \langle \psi_{\tau m} \rangle$ and $F_{D_m} = \langle \psi_{wm} \rangle$ depend on the shape of the waveguide and are expressed in Appendix C for both situations of a tube and a slit.

Note that for a cylindrical tube and a rectangular slit:

$$\psi_{\tau m}(d) = 1 \quad \text{and} \quad \psi_{wm}(d) = 1, \tag{32a}$$

$$\left. \frac{\partial \psi_{\tau m}}{\partial z_3} \right|_d = \frac{V}{S_e} \frac{-j\omega}{\nu'_m} F_{\nu'_m} \quad \text{and} \quad \left. \frac{\partial \psi_{wm}}{\partial z_3} \right|_d = \frac{V}{S_e} \frac{-j\omega}{D_m} F_{D_m}. \tag{32b}$$

By transferring solutions (23) and (24) into boundary conditions (18a-d) and making use of properties (21, 22), we obtain a set of two equations that enable us to determine the integration constants A and B.

1. General expression

Following a lengthy but straightforward calculation, the normalised dynamic compressibility can then be expressed as follows, to the lowest order of ξ, ν' and D:

$$\beta(\omega) \approx 1 + \frac{1}{Q}\left\{\frac{D_m - \nu'_m}{D} F_{\nu'_m} F_{D_m}\left[\gamma - 1 - j\sqrt{\frac{-j\omega}{\nu'}}\xi\Gamma\left(1 - \frac{\gamma-1}{\gamma}h_s\right)\left((\gamma-1)x_v h_L + \gamma k_P\right)\right]\right.$$
$$\left. -\xi\frac{S_e}{V}\left[\gamma k_P \Xi_{D_m} - (\gamma-1)x_a \Xi_{\nu'_m} + (\gamma-1)k_T(1-x_a\alpha_P)(F_{D_m} - F_{\nu'_m})\right]\right\}, \quad (33a)$$

with

$$Q = \left(1 + j\sqrt{\frac{-j\omega}{\nu'}}\xi\Gamma\frac{\gamma-1}{\gamma}h_s h_L x_v\right)\Xi_{D_m} + \frac{D_m - \nu'_m}{D}\left(j\sqrt{\frac{-j\omega}{\nu'}}\frac{V}{S_e}\Gamma F_{\nu'_m} F_{D_m} + \xi\frac{S_e}{V}x_a\right)$$
$$+ j\sqrt{\frac{-j\omega}{\nu'}}\xi\Gamma\left[x_a\Xi_{\nu'_m} - \frac{\gamma-1}{\gamma}k_T(h_L+h_s)(F_{D_m} - F_{\nu'_m})\right], \quad (33b)$$

and

$$\Xi_{D_m} = \left(1 - \frac{\nu'}{D_m}\right)F_{D_m} - \left(1 - \frac{\nu'}{\nu'_m}\right)F_{\nu'_m}, \quad (34a)$$
$$\Xi_{\nu'_m} = \left(1 - \frac{\nu'_m}{D}\right)F_{\nu'_m} - \left(1 - \frac{D_m}{D}\right)F_{D_m}, \quad (34b)$$

As this general expression of the dynamic compressibility involves numerous phenomena from different sources that are coupled together, it is difficult to provide a global interpretation of the physics involved. We thus propose hereafter (§ III B 2) discussions on different specific cases in order to highlight the respective contributions to dynamic compressibility of thermal effects, molecular diffusion, liquid film thickness variations, and heat transfers at the gas-liquid and liquid-solid interfaces.

2. Specific cases

Under the reasonable assumption that the boundary condition (18c) can be reduced to an **isothermal condition** (achieved when $\Gamma \approx 0$), expression (33a) simplifies as follows, accounting for (33b and 34a,b):

$$\beta(\omega) \approx 1 + \frac{1}{Q}\left\{\frac{D_m - \nu'_m}{D}F_{\nu'_m}F_{D_m}(\gamma-1)\right.$$
$$-\xi\frac{S_e}{V}\left[\gamma k_P\Xi_{D_m} - (\gamma-1)x_a\Xi_{\nu'_m}\right.$$
$$\left.\left.+(\gamma-1)k_T(1-x_a\alpha_P)(F_{D_m} - F_{\nu'_m})\right]\right\}, \quad (35a)$$

with

$$Q = \Xi_{D_m} + \frac{D_m - \nu'_m}{D}\xi\frac{S_e}{V}x_a. \quad (35b)$$

The terms related to heat transfers coupled to water phase changes (h_s and h_L) are no longer involved in this expression of $\beta(\omega)$. In this case, **the effects of water evaporation and condensation on the acoustic movement are only related to the displacement of the gas-liquid interface**. This displacement (velocity $\dot{d}$) induces a non-zero acoustic pressure gradient normal to the wall (see eq. 9) that enhances the molecular diffusion of water vapor into dry air (barodiffusion). Considering the orders of magnitude discussed in paragraph II D 3, this result is particularly noteworthy as it highlights the physical phenomena that are expected to have the most significant influence on dynamic compressibility. These aspects are further developed and commented in sections III B 3, IV A 2, V B and V D (eq. 64).

Note that expression (35a) is consistent with previous results in binary gas mixtures without condensed liquid film on the wall[32], by setting $\xi = 0$. In this case, thermodiffusion is the only molecular diffusion process involved, and its contribution to dynamic compressibility is generally negligible compared to that of thermal effects. Therefore, if humid air is considered as a pseudo-pure gas, without molecular diffusion nor condensation phenomena at isothermal boundaries ($k_T = k_P = 0$, $\xi = 0$, $\Gamma = 0$), expression (33a) leads straightforwardly to the well-known expression

$$\beta(\omega) \approx 1 + (\gamma-1)F_{\nu'}. \quad (36)$$

Finally, the **dynamic compressibility of a pure vapor** can also be obtained from expression (33a), in which $x_a = 0$, $D_m = D$, and $\nu'_m = \nu'$, that leads to the following expression, consistent with results available in the literature[9,29],

$$\beta(\omega) \approx 1+ \frac{(\gamma-1)F_{\nu'}\left[1-j\sqrt{\frac{-j\omega}{\nu'}}\xi\Gamma\left(1-\frac{\gamma-1}{\gamma}h_s\right)h_L\right]}{1+j\sqrt{\frac{-j\omega}{\nu'}}\Gamma\left[\frac{V}{S_e}F_{\nu'}+\frac{\gamma-1}{\gamma}h_s h_L\xi\right]}. \quad (37)$$

This expression shows that the effects of evaporation/condensation phenomena on the dynamic compressibility of a vapor in a straight pore are exclusively attributable to heat transfers at the gas–liquid–solid interfaces, which should remain quite low given the expected orders of magnitude for Γ (see section II D 3).

3. *Low frequencies asymptotic behaviour*

Further analysis can be provided by examining the asymptotic behavior of the dynamic compressibility as expressed in eq. (33a) when the thickness of the boundary layers is greater than the pore size. The aim is to identify the physical phenomena that contribute most to the dynamic compressibility when ω tends towards zero. In this case, a **low-frequency expansion of eq. (33a)** simply leads to:

$$\beta(\omega) \xrightarrow[\omega\to 0]{} \gamma\left[1-\frac{S_e}{V}\frac{\xi k_P}{1+\xi\frac{S_e}{V}x_a}\right], \quad (38)$$

where k_P and ξ are given by equations (4) and (18b) respectively.

As the molar mass of water is smaller than that of dry air ($M_a > M_v$), the barodiffusion coefficient is negative (see eq. 4) and the term factor of γ is always greater than 1. Therefore, **water evaporation/condensation phenomena in humid air are expected to increase the static compressibility** of the fluid in the pore.

If there is no liquid film thickness variation ($\xi = 0$), or if molecular diffusion is neglected ($\alpha_P = 0$), the low-frequency normalized compressibility reduces to γ, as expected. It is thus worth noting that the low-frequency value of the compressibility is altered under the effect of molecular diffusion through barodiffusion process (expressed by α_P) activated by the liquid film thickness variation velocity. In fact, the liquid film acts as a vapor source at the boundary whose vibration velocity is coupled to the evaporation/condensation process and mass diffusion in the propagation domain (humid air). As previously outlined, **the acoustic pressure gradient normal to the wall** thus induced is crucial to **amplify water vapor diffusion from the boundary to the bulk of the domain**. Conversely, in the absence of boundary vibration velocity, the water vapor emitted at the boundary remains confined close to it, having a negligible effect on dynamic compressibility.

This key result highlights that the effects of condensation and evaporation processes on acoustic propagation cannot be fully described without taking into account the acoustic behavior of the liquid film coating the wall, as illustrated in Figure 4. This expression also demonstrates that **barodiffusion is the predominant molecular diffusion process at low frequencies**. Finally, **thermodiffusion** (expressed by k_T, and also included in ν'_m and D_m) and **heat transfers at the liquid-gas interface have no effect on the low-frequency dynamic compressibility** (38), i.e. when the boundary layers are large compared to the pore size.

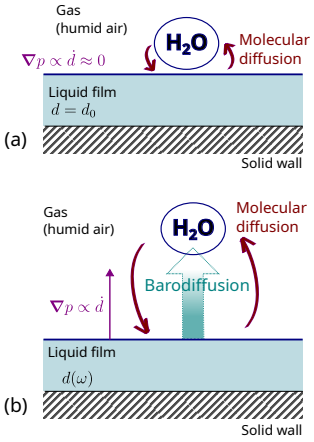

FIG. 4. Schematic view of water evaporation-condensation process: (a) while neglecting the movement of the liquid-gas interface (no barodiffusion); (b) then accounting for the movement of the liquid-gas interface which activates barodiffusion process.

An asymptotic expansion of the expression (33a) of $\beta(\omega)$ can be proposed when the thickness of the boundary layers is small compared to the pore size (high frequencies). However, this asymptotic expansion is rather complex, and identifying main trends from it requires a priori knowledge of the orders of magnitude involved. For the sake of generality, the high-frequency behavior of the dynamic compressibility is thus further discussed after a first analysis of the results presented in section IV B 2.

IV. RESULTS AND DISCUSSIONS

A. Properties of the condensation liquid film

1. *Theoretical expression of the thickness*

We need to express the thickness of the liquid film d as a function of the relative humidity φ (eq. 15). In order to do this, we shall assume that this liquid film is in thermodynamic equilibrium with the water vapor in the environmental conditions under study, namely tempera-

ture T, pressure P and partial pressure of water vapor P_v. This property is expressed by the equality of the chemical potentials of liquid and vapor, leading to the well-known equation

$$\mu_c = \frac{\mathrm{R}T\rho_\ell}{M_v}\ln\left(\frac{P_v}{P_{sv}(T)}\right) = \frac{\mathrm{R}T\rho_\ell}{M_v}\ln(\varphi), \tag{39a}$$

μ_c being the chemical potential by unit mass of water adsorbed by the solid wall and R the universal gas constant.

Furthermore, the expression of the chemical potential μ_c of liquid water coating the solid wall also involves different types of molecular interaction between the water vapor in the air and the solid wall, leading to water vapor adsorption on the wall[31,36]. Due to the polarity of water molecules, these interactions include several kinds of van der Waals forces as well as hydrogen bonds. We see here that the molecular interactions involved are rather complex and depend heavily on the nature, roughness, and geometry of the solid structure. Therefore, it would be an exercise in futility to formally express the function $d(\varphi)$ within a general theoretical framework. Instead, this expression shall be based on available semi-phenomenological models adapted to the porous structure under study[11,31].

In this instance, London forces (i.e. between instantaneous dipoles) should not be the most significant interactions involved. However, one can formally express them in order to obtain a relatively simple expression for the thickness $d(\varphi)$ of a thin liquid film precondensed on a smooth and locally plane solid wall as developed in depth in Ref. 29 and 36. Actually, the thickness of the liquid phase is herein assumed to be large compared with interatomic distances so that this film can be treated as a continuous medium. But this thickness is still assumed to be small enough that it can be expressed as a function of thermodynamic quantities by a relatively simple law, avoiding too complex formula. Finally, the chemical potential μ_c primarily due to London forces can be written as follows

$$\mu_c = \frac{\hbar\overline{\omega}}{8\pi^2 d^3}, \tag{39b}$$

where $\hbar$ is the Planck constant and $\overline{\omega}$ can be interpreted as a complex characteristic frequency for the absorption spectra of the gas, liquid ans solid phases, and related to their complex dielectric constants. By combining equations (39a,b), we are left with

$$d = d_r[-\ln(\varphi)]^{-1/3}, \tag{40}$$

where $d_r^3 = -\frac{\hbar\overline{\omega}M_v}{8\pi^2\mathrm{R}T\rho_\ell}$.

In this expression, which is used by Mehl and Moldover in Ref. 29 to describe the precondensation of propane on a smooth and locally plane metallic wall, the temperature dependence of factor d_r is weak enough to be neglected here. We also use the orders of magnitude given herein, i.e. $d_r = 1\,\mathrm{nm}$, despite their evident inaccuracy for water. According to this approximate expression, the liquid film thickness is expected to be on the order of 5 nm at 99% relative humidity, which is consistent with the usual orders of magnitude encountered in adsorption processes[31]. We therefore consider that expression (40) is sufficient here for identifying general trends and underlying physical phenomena. But the reader is warned that the numerical values presented in section IV may, in some cases, be underestimated. In order to determine a more realistic expression for d, we shall conduct experimental characterizations of adsorption for all porous structures under study. This task will be likely discussed further in a future work.

2. *Specific admittance of the liquid film*

The effect of thickness variation of the liquid film coating the lateral walls of the waveguide ($z_3 = d$) can also be expressed as a specific acoustic admittance on the boundary, defined as follows

$$\zeta_d = \rho_0 c_0 \dot{d}/p(d). \tag{41}$$

We make the simplifying assumption that the value of this specific admittance is small enough to allow us considering a quasi-plane wave propagation in the waveguide, as stated by Bruneau et al[37]

$$|\zeta_d| << \frac{\omega}{c_0}\sqrt{S}. \tag{42}$$

But the reader is warned that, based on (17a) and expression (40) of d, the orders of magnitude obtained for ζ_d as a first approximation indicate that this condition would not be fulfilled in the most severe environmental conditions considered here (see Tab. I). However, these limitations do not affect the general interest of the formalism presented in sections II and III, nor the orders of magnitude and main trends identified hereafter (see § IV B). Further discussions of these limitations together with possible methodologies to address these issues will be examined in a future work.

B. Effective properties of humid air in a cylindrical tube

The results presented in this section are calculated at a fixed atmospheric pressure of 1000 hPa, and for different values of temperature and relative humidity that are listed in Table I. Note that at atmospheric pressure, the expression (40) of $d(\varphi)$ is applicable for temperatures below 100°C.

The main physical properties of humid air and liquid water are computed using the CoolProp library[25], which is validated over a large pressure and temperature range, contrary to methods generally used in acoustics for determining the physical properties of air[24]. As CoolProp does not allow us to compute transport coefficients that

TABLE I. Values of physical quantities describing the state of humid air in four illustrative cases at 1000 hPa static pressure.

	T (°C)	φ (%)	x_v	d_0 (nm)	γ	ρ_0 (kg/m^3)	η (µPa·s)	κ (mW/m/K)	ν (mm^2/s)	ν' (mm^2/s)	D (mm^2/s)	k_T	k_P
atmo. 1	20	50	0.01	1	1.40	1.18	18.1	25.9	15.3	21.6	24.2	-1.4e-3	-4.41e-3
atmo. 2	30	90	0.03	2	1.40	1.13	18.5	26.6	16.3	22.8	25.8	-2.5e-3	-1.42e-2
extreme 1	50	99	0.12	5	1.39	1.03	18.8	27.7	18.2	24.9	29.1	-1.4e-4	-4.27e-2
extreme 2	80	99	0.47	5	1.36	0.81	16.9	27.6	20.7	24.8	34.4	2.2e-2	-1.15e-1

describe molecular diffusion processes, we use expression (4) to calculate the barodiffusion ratio k_P, and the methods given by Hirschfelder[34] for determining the molecular diffusion coefficient D and the thermodiffusion ratio k_T, considering humid air as a binary gas mixture with one polar component. The values of several physical properties of humid air are listed in Table I in the tested environmental conditions. The values for the static liquid layers thickness d_0 are calculated by using eq. (40) and illustrate the expected effects of temperature and water molar fraction on the precondensation process. Note that the signs of the thermo- and barodiffusion ratios express the direction of dry air molecular diffusion into water vapor in response to temperature and pressure gradients, respectively. As shown in eq. (5), the concentration flux density of dry air $\mathbf{i}$ has the same direction than the pressure or temperature gradient if the diffusion ratio is negative.

The results presented in sections IV B 1 and IV B 2 are calculated for a cylindrical tube made of nichrome with a radius of 100 µm, and plotted in the frequency range from 10 Hz to 100 kHz to show clearly the asymptotic behaviors at low and high frequencies.

Finally, the reader is warned that the aim of this section is not to make direct comparisons between the effective properties obtained with the approach presented here and those derived from other modelling procedures available in the literature[8,12]. Remember that these works rely on assumptions differing from the present study, in particular (i) the thermo and barodiffusion are neglected, (ii) the environmental conditions for evaporation/condensation correspond to the saturation point of water, (iii) the thickness and thickness variation of the liquid film is not accounted for. A systematic comparison would thus fall outside the scope of the present work.

1. *Effective density in a cylindrical tube*

As previously discussed (§ III A), condensation/evaporation phenomena have no effect on the effective density of humid air within a cylindrical tube. However, its value may be significantly altered by the physical properties of humid air.

The results obtained for $\rho(\omega)$ with expression (27) and the physical properties listed in Table I are plotted in Figure 5. These results highlight that the effects of temperature and air composition on the effective density of humid air in a cylindrical tube are mainly due to the value of the static density of humid air. Indeed, the kinematic viscosity ν exhibits only small variations (about 7%) under the environmental conditions tested, that leads to minor effects on the imaginary parts. Contrast with this, the environmental conditions considered here lead to higher discrepancies in the density values (more than 30%), with a greater impact on the real parts of the effective density plotted in Fig. 5.

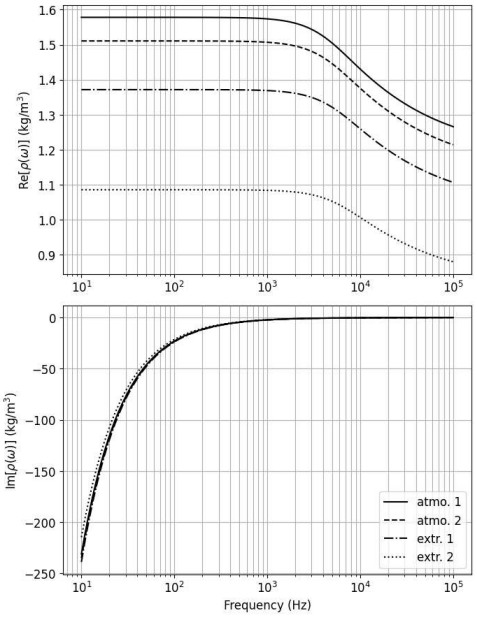

FIG. 5. Effective density vs. frequency (real and imaginary part) at atmospheric pressure and several values of temperature and humidity rate listed in Tab. I.

It could be worth recalling that the asymptotic low frequency behavior of the effective density is governed by viscous effects. By contrast, the asymptotic high frequency behavior is dominated by inertial forces. Around the visco-intertial transition frequency, viscous and inertial behaviors coexist[38].

As outlined in Table I, the effect of water vapor precondensation is expected to be significant in a nanostructured material, based on the orders of magnitude given for the liquid layer static thickness d_0 (i.e. pore cross-section decrease, see for instance Secs. V A 1-2 and 4).

2. *Effective bulk modulus and normalized dynamic compressibility in a cylindrical tube*

In comparison, the value of the effective bulk modulus $K(\omega)$ and normalized dynamic compressibility $\beta(\omega)$ as expressed by eq. (30) and (36) respectively, without condensation and evaporation of water vapour, are less sensitive to the physical properties of humid air as shown in Figure 6.

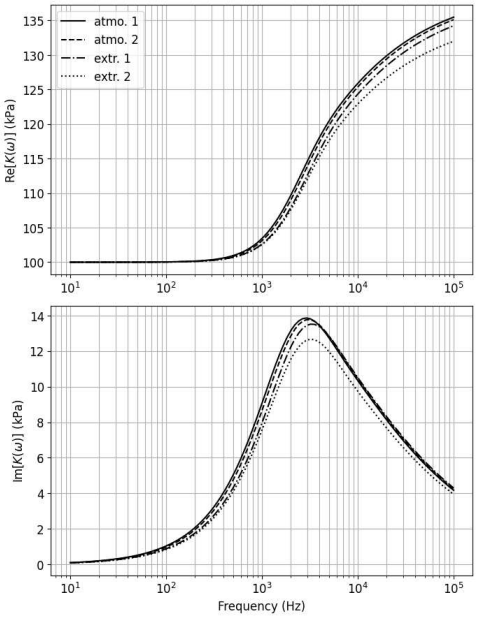

FIG. 6. Effective bulk modulus vs. frequency (real and imaginary parts) at atmospheric pressure and several values of temperature and humidity rate listed in Tab. I (thermal effects only, without precondensation).

Indeed these results are determined at a fixed atmospheric pressure, and the changes in heat capacity ratio are small under the tested ambient conditions (less than 3% variation in γ). However, the transition frequency between isothermal and adiabatic behaviors increases by several hundred hertz (the maximum of the imaginary part is shifted), due to the value of thermal diffusivity, which exhibits about 15% change across the cases considered here.

Regarding the effects of evaporation/condensation phenomena coupled to the acoustic movement on the normalized dynamic compressibility as expressed in eq. (33a), the results obtained under the tested environmental conditions (see Tab. I) are shown in Figure 7 (gray lines). For each environmental condition, the results accounting for thermal effects only are also presented for comparison (black lines).

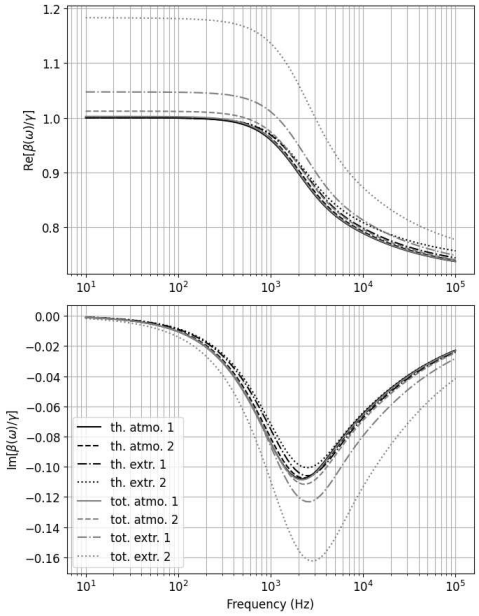

FIG. 7. Dynamic normalized compressibility vs. frequency (real and imaginary parts) at atmospheric pressure and several values of temperature and humidity rate listed in Tab. I (total model with precondensation in grey lines, thermal model without precondensation in black lines).

The **low-frequency asymptotic expansion** (38) is consistent with the results shown in Fig. 7. They highlight the effects of water vapor evaporation/condensation on the boundary coupled with barodiffusion phenomena being significant almost when the water vapor molar fraction x_v is quite high, namely for both "extreme" conditions here. In contrast, under typical atmospheric conditions, these effects remain small (less than 0.25% and 1.2% on the real part of $\beta(0)$ in "atmospheric 1" and "atmospheric 2" conditions respectively) as x_v is of the order of a few 0.01 (see Tab. I).

We propose hereafter a first attempt to identify both the most significant and the negligible phenomena in-

volved in the dynamic compressibility of humid air in a straight pore by analysing the results plotted in Fig. 7 with respect to some specific cases discussed in section III B 2.

Firstly, under the assumption of **isothermal boundary conditions** at the liquid-gas interface, expression (35a) of $\beta(\omega)$ yields relative discrepancies on the real parts less than 0.8%, and 0.004 maximum discrepancies on imaginary parts, compared to expression (38). These maximum discrepancies are reached close to the transition frequency and under environmental conditions that maximize condensation effects (namely 'extreme' conditions). The effect of heat transfers at the solid–liquid–gas interfaces on the dynamic compressibility of humid air in a pore can thus be neglected in many applications.

Furthermore, **in the absence of evaporation/condensation process on the wall**, molecular diffusion phenomena have negligible contribution to the value of $\beta(\omega)$. In this case, we can use the well-known expression (36) as errors thus made are less than 1 ppm.

We also propose to estimate the **contribution of thermodiffusion process to the dynamic compressibility**, as it seems to be low. If we neglect the terms related to thermodiffusion in $\beta(\omega)$ (namely $\alpha_T = 0$, $\nu'_m = \nu'$ and $D_m = D$), which is actually a rough approximation, expression (33a) yields

$$\beta(\omega) \approx 1 - \gamma \frac{\xi \frac{S_e}{V} k_P F_D}{F_D + \xi \frac{S_e}{V} x_a} + (\gamma - 1) F_{\nu'} \,. \qquad (43)$$

The results obtained with this simplified expression (43) are very close to those of expression (33a). Indeed, under 'extreme 2' ambient conditions, relative errors on the real part of the compressibility are less than 1.2%, and discrepancies on the imaginary parts are below 0.006. Under 'extreme 1' conditions, the relative error on the real part is less than 0.1%, and discrepancies on the imaginary part below 0.0004. Therefore, expression (43) should often be sufficient to describe the dynamic compressibility of porous materials saturated with humid air when evaporation/condensation phenomena occur. A formulation of the subsequent simplified acoustic problem is proposed in Appendix D with the derived solutions.

When the thickness of the boundary layers is small compared to the pore size (high frequencies), the asymptotic expansion of expression (43) leads to

$$\beta(\omega) \xrightarrow[\omega\to\infty]{} 1 - \frac{\gamma k_P \xi \frac{S_e}{V}}{1 + \xi x_a \sqrt{\frac{j\omega}{D}}} + (\gamma - 1) \frac{S_e}{V} \sqrt{\frac{\nu'}{j\omega}}. \qquad (44)$$

Beyond 5 kHz and under 'extreme 2' conditions, the discrepancies between this asymptotic expansion (44) and expression (33a) are less than 0.6% in relative values on the real part of dynamic compressibility, and less than 0.06 on the imaginary part. The effects of barodiffusion process coupled to the liquid film thickness variation are small in the high frequency range compared to thermal effects in the boundary layers.

In conclusion, **for many practical cases, especially in environmental conditions close to atmospheric ones, the simplified expression (43) of the dynamic compressibility seems to provide an adapted description of the physical phenomena** coupled to the acoustic movement in humid air-saturated porous media, in which water vapor condensation occurs. Nevertheless, the general expression (33a) of $\beta(\omega)$ remains of fundamental interest when the coupling between thermal and molecular diffusion processes cannot be neglected.

The macroscopic quantities describing acoustic propagation in porous media, in particular dissipative phenomena, are mainly related to visco-inertial effects, which are not affected by precondensation at the walls (except for nanoporous structures, see § III A). Therefore, the specific effects of precondensation remain relatively weak. For instance, regarding the speed of sound in a porous medium, defined as

$$c(\omega) = \sqrt{\frac{K(\omega)}{\rho(\omega)}}, \qquad (45)$$

precondensation processes should result in reducing its low-frequency value of approximately 8% in the most extreme environmental condition studied ("extreme 2"). Therefore, the impact of precondensation on acoustic propagation in a porous medium should be low in most cases, but significant under extreme temperature and humidity conditions.

Finally, let us briefly comment on the influence of static pressure P_0 on molecular diffusion processes, which is indeed not considered in the results presented herein. In fact, molecular diffusion processes are known to decrease as molecules get close to each other, which is expressed by the molecular diffusion coefficient D being inversely proportional to P_0[34]. Consequently, all physical phenomena related to molecular diffusion of water vapor described in the present work are expected to have lower effects on the acoustic propagation in porous media for applications requiring high working static pressures.

V. GENERALIZATION TO POROUS MATERIALS WITH STRAIGHT PORES

The aim of this section is *(i)* to provide an overview of the intrinsic parameters and quantities generally used to describe the properties of porous media, and *(ii)* to detail the dynamic quantities that are significantly altered by the condensation and evaporation process coupled to the acoustic movement, namely the dynamic thermal permeability and compressibility.

Detailed quantitative results would be the subject of future works, taking advantage of this adapted formulation and of the attached discussion. It is beyond the scope of this paper.

A. Intrinsic parameters and quantities describing the physical properties of porous media

We recall here the basic definitions of the key macroscopic parameters that are typically used to describe porous media in order to highlight the impact of condensation and evaporation processes on each one.

1. Porosity

The porosity ϕ is defined as the ratio of the fluid volume V to the total volume of the material V_t, that can also be expressed as follows by introducing the homogenisation volume Ω and the fluid volume Ω_f:

$$\phi = \frac{V}{V_t} = \frac{1}{\Omega}\int_{\Omega_f} 1\,\mathrm{d}\Omega = \frac{\Omega_f}{\Omega}, \tag{46}$$

where $\frac{1}{\Omega}\int_{\Omega_f}\cdot\,\mathrm{d}\Omega$ denoted $\langle\cdot\rangle_\Omega$ is the averaging operator over the homogenisation volume Ω.

For the purpose of this work, the averaging operator over the fluid volume Ω_f is defined as[39]

$$\langle\cdot\rangle = \frac{1}{\Omega_f}\int_{\Omega_f}\cdot\,\mathrm{d}\Omega = \frac{1}{\phi}\langle\cdot\rangle_\Omega, \tag{47}$$

which is formally equivalent to the averaging operator over the cross-section of the pore defined in eq. (25). The respective expressions of the F_X terms remain thus unchanged (see Appendix C).

Note that only the volume of fluid which is not locked within the frame must be considered in Ω_f and thus in the calculation of the porosity (open or connected porosity).

Water condensation within the material is expected to decrease the volume Ω_f, and thus the porosity ϕ. The static thickness d_0 of the liquid film condensed on the pore walls being on the order of a few nanometers (see Table I), the effects of condensation on porosity should be negligible as long as the pores sizes are much larger than d_0.

2. Viscous permeability

One of the important parameters governing the absorption of a porous material is its static viscous permeability k_0, which is described by means of the Darcy law

$$\boldsymbol{U} = -\frac{k_0}{\eta}\boldsymbol{\nabla} P, \tag{48}$$

for a quasi-static fluid flow of average velocity $\boldsymbol{U}$ and submitted to a pressure gradient $\boldsymbol{\nabla} P$.

For a dynamic flow (angular frequency ω) within a porous volume Ω of porosity ϕ, that involves the mean particle velocity $\langle\mathbf{v}_{12}\rangle_\Omega$ and the pressure gradient $\boldsymbol{\nabla}_{12} p$, expressions (26) and (27) lead to the following relationship as given by Johnson[26]:

$$\langle\mathbf{v}_{12}\rangle_\Omega = \phi\langle\mathbf{v}_{12}\rangle = -\frac{k(\omega)}{\eta}\boldsymbol{\nabla}_{12} p \tag{49}$$

the dynamic viscous permeability being given by

$$k(\omega) = \frac{\phi\nu}{j\omega}(1 - F_\nu), \tag{50}$$

in which F_ν depends on the shape of the pores and involves visco-inertial effects only (see Appendix C).

The static permeability k_0 is given by the low-frequency limit of $k(\omega)$ and depends on the pore geometry (intrinsic property). In particular, for a material with cylindrical pores (radius R), $k_0 = \phi R^2/8$ as shown in reference 26. Consequently, k_0 is altered by water condensation on walls only through a pore cross-section decrease, this effect being negligible when the pore size is much larger than the static thickness d_0 of the liquid film coating the walls.

Moreover, expression (50) of the dynamic viscous permeability shows that $k(\omega)$ does not depend on the condensation and evaporation phenomena occurring during an acoustic cycle. However, dynamic permeability of a porous material remains a function of the physical properties of humid air (related to P_0, T_0 and φ), like its effective density (see eq. 27).

3. Tortuosity

The dynamic tortuosity $\alpha(\omega)$ is defined by Johnson et al[26] from a generalization of the response of a non-viscous fluid to a pressure gradient (Euler's law)

$$j\omega\alpha(\omega)\rho_0\langle\mathbf{v}_{12}\rangle = -\boldsymbol{\nabla}_{12} p, \tag{51}$$

that leads, by identification with eq. (49), to

$$\alpha(\omega) = \frac{\phi\eta}{j\omega k(\omega)\rho_0}. \tag{52}$$

For a non-viscous fluid, the tortuosity value α_∞ is given by the high-frequency limit of $\alpha(\omega)$. This real quantity depends on the geometry of pores only. This intrinsic parameter α_∞ quantifies the dispersion of the particle velocity $\mathbf{v}_\infty$ in the non-viscous fluid due to pores diameter variations:

$$\alpha_\infty = \frac{\langle\mathbf{v}_\infty\cdot\mathbf{v}_\infty\rangle}{\langle\mathbf{v}_\infty\rangle\cdot\langle\mathbf{v}_\infty\rangle} \geq 1. \tag{53}$$

The relationship (52) between tortuosity and dynamic viscous permeability implies that water vapor condensation/evaporation process should have no effect on α_∞ and $\alpha(\omega)$, except through geometric alterations of the pores (such as diameter decrease, localized liquid water accumulation within the pore network, or roughness smoothing). Actually, these effects will be negligible if the pores sizes are large compared to d_0. However, as for viscous permeability and effective density, the dynamic tortuosity do depend on the physical properties of humid air.

4. Viscous characteristic length

It has been shown by Johnson et al[40] that the high-frequency behavior of the dynamic viscous permeability $k(\omega \to \infty)$ depends on the viscous characteristic length defined by

$$\Lambda = 2\frac{\int_{\Omega_f} \mathbf{v}_\infty \cdot \mathbf{v}_\infty \mathrm{d}\Omega}{\int_{\partial\Omega_f} \mathbf{v}_\infty \cdot \mathbf{v}_\infty \mathrm{d}\partial\Omega}, \tag{54}$$

$\partial\Omega_f$ being the surface enclosing the fluid domain.

The viscous characteristic length Λ is generally an effective pore-volume-to-surface ratio, in which each volume or area element is weighted according to the local value of the velocity field $\mathbf{v}_\infty$. This weighting eliminates contributions from the isolated regions of the pore space that do not contribute to transport. The characteristic length Λ is an intrinsic measure of an interconnected pore radius. For a straight cylindrical waveguide with constant cross-section, Λ is equal to its radius R.

Thus, the condensation of a liquid film on the solid walls of a porous material will simply lead to a slight reduction of the hydraulic radius of pores, that is negligible when this radius is large respect to the thickness of the liquid film.

5. Thermal characteristic length

It has been shown by Champoux and Allard[27] that the high-frequency behavior of the bulk modulus $K(\omega \to \infty)$ can be characterized by a second characteristic length given by

$$\Lambda' = 2\frac{\int_{\Omega_f} \mathrm{d}\Omega}{\int_{\partial\Omega_f} \mathrm{d}\partial\Omega} = \frac{2\Omega_f}{\partial\Omega_f} = \frac{2V}{S_e}. \tag{55}$$

In dry porous media having identical cylindrical pores, $\Lambda' = \Lambda = R$. A liquid layer coating pores walls will thus have the same effects on both viscous and thermal characteristic lengths Λ and Λ' as discussed above (§ V A 4).

6. Static thermal permeability

The static thermal permeability k'_0 plays, in the description of the thermal exchanges between the frame and saturating fluid, a role similar to the viscous permeability k_0 in the description of the viscous forces. When the frame has a sufficient thermal capacity for the compressibility $\beta(\omega)$ to reach the value γ at low frequencies, the temperature variation τ is subjected to isothermal conditions at the pore walls. The static thermal permeability k'_0 is a real constant related to the trapping constant of the frame[41]. It can be predicted analytically for simple geometries[42], in particular for porous media having identical cylindrical pores $k'_0 = k_0 = \phi R^2/8$. Thus k'_0 is impacted by liquid water condensation in the same way as the other intrinsic parameters listed above (i.e. pores size reduction, which is negligible if d is small).

The results obtained in section IV for a straight waveguide with constant cross-section highlight that the dynamic thermal properties of porous media should be significantly altered by successive evaporation and condensation phenomena during an acoustic cycle. Accordingly, these effects on thermal permeability and dynamic compressibility are detailed hereafter.

B. Dynamic thermal permeability

The thermal dynamic permeability $k'(\omega)$ is defined by analogy with the viscous dynamic permeability (49) through the mean value of expression (23) for the variable τ, so that[28]

$$\langle\tau\rangle_\Omega = j\omega\frac{k'(\omega)}{\kappa}p, \tag{56}$$

in which

$$k'(\omega) = \frac{\phi\nu'}{j\omega}(1 - AF_{\nu'_m} - BF_{D_m}), \tag{57}$$

A and B coefficients being expressed as functions of $F_{\nu'_m}$ and F_{D_m} (see § III B).

The usual definition of thermal permeability implies isothermal boundary conditions, which is often a reasonable assumption as illustrated by the results discussed above (see § IV). Thus, we assume $\Gamma = 0$ hereafter, and we obtain the following expression

$$k'(\omega) = \frac{\phi\nu'}{j\omega}\left[1 - \frac{\frac{D_m-\nu'_m}{D}F_{D_m}F_{\nu'_m} + \xi\frac{S_e}{V}x_a[\Xi_{\nu'_m} - x_v\alpha_T(F_{D_m} - F_{\nu'_m})]}{\Xi_{D_m} + \frac{D_m-\nu'_m}{D}\xi\frac{S_e}{V}x_a}\right]. \tag{58}$$

This expression primarily involves two phenomena coupled with thermal effects:

- the liquid film thickness variation, expressed by the terms involving ξ (see eq. 18b),
- the molecular thermodiffusion processes, expressed by the terms involving α_T, D_m, ν'_m (see eq. 21).

Note that the barodiffusion process, expressed by the barodiffusion ratio k_P, does not appear in the expression for dynamic thermal permeability. Indeed, the definition of $k'(\omega)$ is based on the mean value of the temperature variation field expressed in eq. (23) which does not involve barodiffusion process. Furthermore, the results presented in section IV show that thermodiffusion phenomena clearly have minor effects on acoustic propagation in humid air filled waveguides. Seeing this, we should not be

surprised to find that evaporation/condensation process has negligible effects on the dynamic thermal permeability of humid air saturated porous media.

Let us now attempt to identify the low- and high-frequency behaviors of the dynamic thermal permeability, on which are based the static thermal permeability and the thermal characteristic length respectively.

First, the **low-frequency limit of expression (58)** yields

$$k'(\omega) \xrightarrow[\omega\to 0]{} \frac{R^2}{8}\phi\frac{1+\xi\frac{S_e}{V}x_a(1+x_v\alpha_T)}{1+\xi\frac{S_e}{V}x_a},$$

in which we identify the static thermal permeability $k'_0 = \frac{R^2}{8}\phi$ defined in section V A 6, as expected. This low-frequency limit of $k'(\omega)$ is however modified here by a real factor that expresses the coupling between the liquid film on the wall and thermodiffusion phenomena.

The sign of α_T describe the direction of dry air thermodiffusion process into water vapor, which depends on the environmental conditions. Therefore, we cannot generally state whether the low-frequency thermal permeability should increase or decrease under the effect of evaporation/condensation. Anyway, $|x_v\alpha_T|$ **is expected to be negligible in humid air**, according to the values of thermodiffusion ratio given in Table I, leading thus to

$$k'(\omega) \xrightarrow[\omega\to 0]{} k'_0\frac{1+\xi\frac{S_e}{V}x_a(1+x_v\alpha_T)}{1+\xi\frac{S_e}{V}x_a} \approx k'_0 \qquad (59)$$

On the other hand, when the thickness of boundary layers is small respect to the pore size, the **high-frequency asymptotic expansion of expression (58)** is written as

$$k'(\omega) \xrightarrow[\omega\to\infty]{} \frac{\phi\nu'}{j\omega}\left[1-(1-j)\frac{\delta'}{\Lambda'}\frac{\sqrt{\nu'}+\sqrt{D}\left[1+\sqrt{\frac{D}{\nu'}}(\epsilon-x_v\alpha_T)\right]}{\sqrt{\nu'_m}+\sqrt{D_m}}\right]. \qquad (60)$$

One more time, the asymptotic behavior thus obtained slightly differs from those expected due to the factor of δ'/Λ'. Since $\epsilon < |x_v\alpha_T| \ll 1$, which also implies $\nu'_m \approx \nu'$ and $D_m \approx D$, this factor approaches unity, thereby yielding **negligible effects on the high-frequency thermal permeability**.

C. Normalized dynamic compressibility

Finally, we can identify a relationship between the normalized dynamic compressibility and the dynamic thermal permeability, as previously established by Lafarge[28]. The key difference here is that the compressibility of the air within the pores is modified by molecular diffusion, expressed through the concentration variation w.

Thus, the average value over Ω of eq. (6a), accounting for (24), (56), and (57), leads to

$$-\boldsymbol{\nabla}_{12}\langle\mathbf{v}_{12}\rangle_\Omega = j\omega\frac{\phi\beta(\omega)}{\gamma P_0}p, \qquad (61)$$

where the dynamic compressibility takes the following form, consistent with eq. (35a),

$$\beta(\omega) = \gamma\left[1-k_P\xi\frac{S_e}{V}\frac{\Xi_{D_m}-\frac{\gamma-1}{\gamma}x_a\alpha_T(F_{D_m}-F_{\nu'_m})}{\Xi_{D_m}+\xi\frac{S_e}{V}x_a\frac{D_m-\nu'_m}{D}}\right] - (\gamma-1)\frac{j\omega}{\nu'}\frac{k'(\omega)}{\phi}. \qquad (62)$$

Let us take a closer look at this key result by considering first the right-hand side of the mass conservation equation (6a), which is derived from the equation of state expressing the thermodynamic equilibrium of humid air, i.e. a dry air-water vapor mixture. In a pure (or pseudo-pure) gas, acoustic pressure involves density and temperature variations only and the dynamic compressibility is given by the well-known expression[28]

$$\beta(\omega) = \gamma - (\gamma-1)\frac{j\omega}{\nu'}\frac{k'(\omega)}{\phi}. \qquad (63)$$

In a binary gas mixture submitted to an acoustic pressure p, a concentration variation w is also involved through barodiffusion process. When one component of the mixture is a saturated vapor, barodiffusion is enhanced by the vibration velocity imposed on the boundary by the thickness variation of the liquid film due to vapor evaporation and condensation during an acoustic cycle, as explained in section IV B 2.

Furthermore, remember that the temperature variation τ is also coupled to the concentration variation, but only through thermodiffusion process, which has been seen to be negligible for most applications in humid air.

According to this, we should not be surprised to find that the dynamic compressibility $\beta(\omega)$ of humid air-saturated porous media (62) is impacted by molecular diffusion phenomena coupled with the liquid film thickness variation, whereas the dynamic thermal permeability $k'(\omega)$ is not significantly altered (see eq. 58).

D. Summary

In summary, **the macroscopic geometric parameters** (porosity ϕ, thermal characteristic length Λ') **and asymptotic parameters** (tortuosity α_∞, viscous characteristic length Λ, viscous and thermal permeabilities k_0 and k'_0) should not be affected by adsorption phenomena as long as the pore sizes remain large compared to the thickness of the liquid film formed on the wall, which should not exceed a few tenth of nanometers. This therefore applies to all materials that do not have a nanostructure.

The dynamic permeability $k(\omega)$ should also not be affected by the dynamic phenomena associated with the precondensation of water vapor in the pore walls. This reasoning can presumably be generalized to any porous structure, allowing $k(\omega)$ to be expressed as proposed by Johnson et al.[26] [Eq. (3.4ab)].

The dynamic thermal permeability $k'(\omega)$ is formally impacted by the presence of water vapor thermodiffusion processes in the air [Eq. (58)]. However, numerical applications indicate that these phenomena have no significant effect in the case of humid air, even under extreme environmental conditions. Consequently, it seems reasonable to assume that these considerations can also be generalized to any porous structure and that $k'(\omega)$ can always be expressed as proposed by Lafarge et al.[28] [Eq. (22)].

Finally, **only the normalized dynamic compressibility $\beta(\omega)$ should be significantly affected by barodiffusion phenomena activated by the variation in the thickness of the liquid film at the wall, with the effects of thermodiffusion remaining quantitatively negligible**. Thus, expression (62), valid for a straight pore, can be simplified as follows, assuming $\alpha_T = 0$,

$$\beta(\omega) = \gamma \left(1 - k_P \xi \frac{S_e}{V} \frac{F_D}{F_D + \xi \frac{S_e}{V} x_a}\right) - (\gamma - 1) \frac{j\omega}{\nu'} \frac{k'(\omega)}{\phi}, \tag{64}$$

where F_D and S_e/V are related to the cross-sectional shape of the straight pore. These terms are explicitly given in Appendix C for a circular cross-section and a slit, but this expression (64) of $\beta(\omega)$ should be generalizable to other cross-section shapes by using appropriate forms for F_D and S_e/V, such as those proposed, for example, by Stinson[43].

VI. CONCLUSION

The main objective of this work was to improve the understanding of physical phenomena coupled to the acoustic field in humid air-saturated porous media. For this purpose, we have proposed a formulation of the acoustic problem, in which humid air is considered as a binary gas mixture of dry air and water vapor, the latter being likely to precondense on a solid wall. Analytical solutions are given for a straight pore, and illustrated by theoretical results obtained on a cylindrical geometry under different environmental conditions.

These results highlight the physical phenomena that most significantly alter viscous and thermal dissipative processes in acoustic materials. First, environmental conditions have a significant effect on the effective dynamic density of the equivalent fluid. Furthermore, under extreme environmental conditions, successive evaporation/condensation of water vapor on the wall results in increasing the low-frequency value of the normalized dynamic compressibility. This is mainly due to the barodiffusion of water vapor in the air, activated by the vibration velocity imposed by the thickness variation of the adsorbed liquid film at the boundary of the propagation domain. Having noticed that this phenomenon dominates over the others, it is straightforward to simplify the solutions but also the formulation of the acoustic problem (see Appendix D which could also be particularly useful for numerical implementations when dealing with more complex microstructures).

In practice, based on these results, we provide guidelines for generalizing the proposed formalism to the study of porous media. Phenomena specifically related to water vapor precondensation should not alter the intrinsic geometric and asymptotic properties of a porous material, except nanostructured ones. Should the environmental conditions be such that the effects of precondensation are significant, an analytical expression is proposed for the dynamic compressibility of straight-pores materials.

However, it is worth noting that the theoretical approach proposed here is subject to several limitations. In particular, the thermodynamic behavior of the liquid film on the wall shall be expressed on the basis of experimental characterizations on the porous structures under study, and semi-phenomenological models available to describe adsorption processes (see discussion § IV A 1). This will also enable us to better assess the plane wavefront perturbations due to the non-zero admittance of the liquid film on the wall, as mentioned in section IV A 2.

Further research is also required to carry out a systematic comparison with existing theoretical approaches developed for addressing similar issues[8,12], in order to identify the experimental conditions that would enable us to highlight the main physical phenomena and consistent modeling assumptions.

The results obtained illustrate that the application areas in which the models developed here can be fully exploited are likely to extend beyond the fields of conventional airborne acoustics, as the effects of precondensation on acoustic propagation in porous media are only significant outside atmospheric conditions. Therefore, the optimization of thermoacoustic machines with wet stacks remains a key application of this work, which shall require accounting for a static temperature gradient along the stack. The design of acoustic absorbers adapted to harsh environments would also be a possible application. Finally, the design of smart architected materials, especially humidity-sensitive acoustic metamaterials, or new sensor concepts shall also be considered.

ACKNOWLEDGMENTS

This work was supported by the Région Normandie and LabEx EMC3 of Normandie Université through AMPHI and CarAc projects respectively. We would also like to thank Dr. Rodolfo Venegas for useful conversations.

Appendix A: Thermal diffusion at the gas-liquid-solid interfaces

The temperature variation normal to the wall inside the liquid film (z_3 direction) is expressed as follows ($\sqrt{-j} = e^{-j\pi/4}$):

$$\tau_\ell(z_3) = A_\ell \exp j\sqrt{-j\omega\frac{\rho_\ell C_\ell}{\kappa_\ell}}\, z_3 + B_\ell \exp -j\sqrt{-j\omega\frac{\rho_\ell C_\ell}{\kappa_\ell}}\, z_3, \tag{A1}$$

κ_ℓ and C_ℓ being respectively the thermal conductivity and heat capacity of liquid water. The coefficients A_ℓ, B_ℓ are determined hereafter. Moreover, the temperature variation in the solid wall, that is supposed here to vanish for $z_3 \to -\infty$, is written

$$\tau_s(z_3) = A_s \exp j\sqrt{-j\omega\frac{\rho_s C_s}{\kappa_s}}\, z_3, \tag{A2}$$

where ρ_s, C_s, κ_s are respectively the mass density, the heat capacity and the thermal conductivity of the solid wall. The continuity of temperature variations and heat flux at the liquid-solid interface ($z_3 = 0$) lead straightforwardly to

$$\tau_\ell(z_3) = A_s\left[\cos\sqrt{-j\omega\frac{\rho_\ell C_\ell}{\kappa_\ell}}\, z_3 + j\Theta\sin\sqrt{-j\omega\frac{\rho_\ell C_\ell}{\kappa_\ell}}\, z_3\right], \tag{A3}$$

with

$$\Theta = \sqrt{\frac{\rho_s C_s \kappa_s}{\rho_\ell C_\ell \kappa_\ell}}. \tag{A4}$$

The continuity of temperature variation at the liquid-gas interface ($z_3 = d$) allows us to remove A_s from the previous expression of $\tau_\ell(z_3)$ as follows

$$\tau_\ell(z_3) = \tau(d)\frac{\cos\sqrt{-j\omega\frac{\rho_\ell C_\ell}{\kappa_\ell}}\, z_3 + j\Theta\sin\sqrt{-j\omega\frac{\rho_\ell C_\ell}{\kappa_\ell}}\, z_3}{\cos\sqrt{-j\omega\frac{\rho_\ell C_\ell}{\kappa_\ell}}\, d + j\Theta\sin\sqrt{-j\omega\frac{\rho_\ell C_\ell}{\kappa_\ell}}\, d}. \tag{A5}$$

Finally, we derive from this the following expression of the heat flux $q_\ell(z_3)$ in the liquid film

$$q_\ell(z_3) = -\kappa_\ell \left.\frac{\partial\,\tau_\ell}{\partial z_3}\right|_d = -j\sqrt{-j\omega\rho_0 C_P \kappa}\frac{\tau(d)}{\Gamma} \tag{A6}$$

with

$$\Gamma = \sqrt{\frac{\rho_0 C_P \kappa}{\rho_\ell C_\ell \kappa_\ell}}\frac{1 + j\Theta\tan\sqrt{-j\omega\frac{\rho_\ell C_\ell}{\kappa_\ell}}d}{j\tan\sqrt{-j\omega\frac{\rho_\ell C_\ell}{\kappa_\ell}}d + \Theta}. \tag{A7}$$

It is worth noting that when the thickness of the liquid film d is very small, Γ expresses the contrast between humid air and solid wall thermal properties:

$$\lim_{d\to 0}\Gamma = \sqrt{\frac{\rho_0 C_P \kappa}{\rho_s C_s \kappa_s}}.$$

Appendix B: Liquid film thickness variation

According to expression (15) of φ, we can write the partial derivatives involved in the expression of $\dot{d}$ (16) as follows

$$\left(\frac{\partial\,\varphi}{\partial T}\right)_{P_0,W_0} = -\frac{x_v P_0}{P_{sv0}^2}\left(\frac{\partial\,P_{sv}}{\partial T}\right)_{P_0,T_0}, \tag{B1a}$$

$$\left(\frac{\partial\,\varphi}{\partial W}\right)_{P_0,T_0} = -\frac{P_0}{P_{sv0}}\frac{M^2}{M_a M_v}, \tag{B1b}$$

$$\left(\frac{\partial\,\varphi}{\partial P}\right)_{T,W} = \frac{x_v}{P_{sv0}}\left[1 - \frac{P_0}{f_v}\left(\frac{\partial\,f_v}{\partial P}\right)_{T_0}\right] \approx \frac{x_v}{P_{sv0}}, \tag{B1c}$$

where $P_{sv0} = f_v(P_0, T_0)P_s(T_0)$, the pressure P having minor effects on the enhancement factor $f_v(P, T)$.

Appendix C: Expressions of functions $\psi_{\tau m}$ and ψ_{wm} and coefficients $F_{\nu'_m}$ and F_{D_m}

1. Cylindrical tube

We consider here a cylindrical duct of nominal radius R_0 and effective radius $R = R_0 - d_0$ accounting for a condensation film of static thickness d_0, in the (r, θ, z) cylindrical coordinates. The functions $\psi_{\tau m}(z_3)$ and $\psi_{wm}(z_3)$ are given by the Bessel functions of the first kind as follows

$$\psi_{\tau m}(z_3) = \frac{J_0\left(\sqrt{\frac{-j\omega}{\nu'_m}}r\right)}{J_0\left(\sqrt{\frac{-j\omega}{\nu'_m}}R\right)}, \quad \psi_{wm}(z_3) = \frac{J_0\left(\sqrt{\frac{-j\omega}{D_m}}r\right)}{J_0\left(\sqrt{\frac{-j\omega}{D_m}}R\right)}, \tag{C1}$$

that leads to the following expressions for the mean values $F_{\nu'_m}$ and F_{D_m} of functions $\psi_{\tau m}(z_3)$ and $\psi_{wm}(z_3)$ respectively:

$$F_{\nu'_m} = \frac{2}{R}\sqrt{\frac{\nu'_m}{-j\omega}}\frac{J_1\left(\sqrt{\frac{-j\omega}{\nu'_m}}R\right)}{J_0\left(\sqrt{\frac{-j\omega}{\nu'_m}}R\right)}, \tag{C2a}$$

and

$$F_{D_m} = \frac{2}{R}\sqrt{\frac{D_m}{-j\omega}}\frac{J_1\left(\sqrt{\frac{-j\omega}{D_m}}R\right)}{J_0\left(\sqrt{\frac{-j\omega}{D_m}}R\right)}. \tag{C2b}$$

In the (r, θ, z) cylindrical coordinates, the first derivatives of functions $\psi_{\tau m}(z_3)$ and $\psi_{wm}(z_3)$ with respect to z_3 at the gas/liquid interface ($z_3 = d$ or $r = R$) are thus given by

$$\left.\frac{\partial\psi_{\tau m}}{\partial z_3}\right|_d = -\left.\frac{\partial\psi_{\tau m}}{\partial r}\right|_R = \frac{-j\omega}{\nu'_m}\frac{R}{2}F_{\nu'_m}, \tag{C3a}$$

and

$$\left.\frac{\partial\psi_{wm}}{\partial z_3}\right|_d = -\left.\frac{\partial\psi_{wm}}{\partial r}\right|_R = \frac{-j\omega}{D_m}\frac{R}{2}F_{D_m}, \tag{C3b}$$

the ratio $R/2$ being equal to the volume/surface ratio V/S_e.

2. Rectangular slit

In a rectangular slit of nominal thickness h_0 and effective thickness $h = h_0 - 2d_0$ accounting for a condensation film of static thickness d_0, in the (x, y, z) coordinates, the functions $\psi_{\tau m}(z_3)$ and $\psi_{wm}(z_3)$ are given by

$$\psi_{\tau m}(z_3) = \frac{\cos\sqrt{\frac{-j\omega}{\nu'_m}}(z - h/2)}{\cos\sqrt{\frac{-j\omega}{\nu'_m}}h/2}\,, \tag{C4a}$$

$$\psi_{wm}(z_3) = \frac{\cos\sqrt{\frac{-j\omega}{D_m}}(z - h/2)}{\cos\sqrt{\frac{-j\omega}{D_m}}h/2}\,, \tag{C4b}$$

that leads to the following expressions for the mean values $F_{\nu'_m}$ and F_{D_m} of functions $\psi_{\tau m}(z_3)$ and $\psi_{wm}(z_3)$ respectively:

$$F_{\nu'_m} = \frac{2}{h}\sqrt{\frac{\nu'_m}{-j\omega}}\tan\left(\sqrt{\frac{-j\omega}{\nu'_m}}\frac{h}{2}\right)\,, \tag{C5a}$$

and

$$F_{D_m} = \frac{2}{h}\sqrt{\frac{D_m}{-j\omega}}\tan\left(\sqrt{\frac{-j\omega}{D_m}}\frac{h}{2}\right). \tag{C5b}$$

In the (x, y, z) coordinates, the first derivatives of functions $\psi_{\tau m}(z_3)$ and $\psi_{wm}(z_3)$ with respect to z_3 at the gas/liquid interface ($z_3 = d$ or $x = 0$, $x = h$) are thus given by

$$\left.\frac{\partial\psi_{\tau m}}{\partial z_3}\right|_d = \left.\frac{\partial\psi_{\tau m}}{\partial x}\right|_0 = -\left.\frac{\partial\psi_{\tau m}}{\partial x}\right|_h = \frac{-j\omega}{\nu'_m}\frac{h}{2}F_{\nu'_m}\,, \tag{C6a}$$

and

$$\left.\frac{\partial\psi_{wm}}{\partial z_3}\right|_d = \left.\frac{\partial\psi_{wm}}{\partial x}\right|_0 = -\left.\frac{\partial\psi_{wm}}{\partial x}\right|_h = \frac{-j\omega}{D_m}\frac{h}{2}F_{D_m}\,, \tag{C6b}$$

the ratio $h/2$ being equal to the volume/surface ratio V/S_e.

Appendix D: Acoustic problem without considering thermodiffusion process

In section II, we propose a general formulation of the acoustic problem, accounting for thermodiffusion process and heat transfers at the as-liquid-solid interfaces, whose respective contributions have been demonstrated to be negligible in practice (see § IV). In this Appendix, these phenomena are neglected. This provides the reader with a boundary value problem that is more suitable to be solved for porous medium consisting of complex microstructures.

The equations of acoustics in a gas-vapor mixture eq. (6a-d) are simplified as follows when the molecular thermodiffusion process is neglected:

$$\frac{\partial}{\partial z_3}v_3 + \boldsymbol{\nabla}_{12}\cdot\mathbf{v}_{12} = -j\omega\left(\frac{p}{P_0} - \frac{\tau}{T_0} - \alpha_P\frac{M^2}{M_aM_v}w\right)\,, \tag{D1a}$$

$$j\omega\rho_0\mathbf{v}_{12} = -\boldsymbol{\nabla}_{12}p + \eta\frac{\partial^2}{\partial z_3^2}\mathbf{v}_{12}\,, \tag{D1b}$$

$$j\omega\rho_0C_P\tau = \kappa\Delta\tau + j\omega p\,, \tag{D1c}$$

$$j\omega w = D\Delta w + D\frac{M_aM_v}{M^2}\frac{k_P}{P_0}\Delta p\,. \tag{D1d}$$

Consequently, the concentration variation w is only coupled to the pressure variation p (through barodiffusion process) and not to the temperature variation τ.

Moreover, if we neglect heat transfers at the solid-liquid-gas interfaces, the boundary conditions (18a-c) on the temperature and concentration variations τ and w respectively are simplified as follows:

$$\frac{M^2}{M_aM_v}\left.\frac{\partial w}{\partial z_3}\right|_d = -\frac{j\omega}{D}x_a\xi\left[x_v\frac{p(d)}{P_0} - \frac{M^2}{M_aM_v}w(d)\right], \tag{D2a}$$

which involves the coupling between pressure, concentration and liquid film thickness variations, and

$$\tau(d) = 0. \tag{D2b}$$

In a waveguide, the solution of this acoustic problem for the particle velocity remains as expressed in eq. (20).

The solution (23) for the temperature variation is reduced to the usual expression in thermo-viscous fluids:

$$\tau(z_1, z_2, z_3) = \frac{p(z_1, z_2)}{\rho_0C_P}[1 - \psi_\tau(z_3)]\,, \tag{D3}$$

the function $\psi_\tau(z_3)$ being written as $\psi_{\tau m}(z_3)$ (see Appendix C) in which ν'_m is replaced by ν'.

The solution (24) for the concentration variation is given by

$$w(z_1, z_2, z_3) = \frac{M_aM_v}{M^2}\frac{k_P}{P_0}\frac{D}{j\omega}\Delta p[1 - B_0\psi_w(z_3)]\,, \tag{D4}$$

the function $\psi_w(z_3)$ being written as $\psi_{wm}(z_3)$ (cf. Appendix C) in which D_m is replaced by D, and the constant B_0 being determined by the boundary condition (D2a). At the lowest order of approximation, we assume $\Delta p \approx -\frac{\omega^2}{c_0^2}p$, which leads to

$$B_0 = x_a\frac{S_e}{V}\xi\frac{1 - \frac{c_0^2}{j\omega D}\frac{x_v}{k_P}}{F_D + x_a\frac{S_e}{V}\xi}. \tag{D5}$$

Therefore, we make the same simplifying assumptions as in section III B and we derive from mass conservation equation (D1a) the following relationship:

$$-\boldsymbol{\nabla}_{12} \cdot \langle \mathbf{v}_{12} \rangle = j\omega \frac{\beta(\omega)}{\gamma P_0} p, \tag{D6}$$

in which the normalized dynamic compressibility is given by

$$\beta(\omega) = 1 + (\gamma - 1) F_{\nu'} - \gamma k_P \xi \frac{S_e}{V} \frac{F_D}{F_D + x_a \frac{S_e}{V} \xi}, \tag{D7}$$

at the lowest order of approximation, which is consistent with the simplified expression (43) of $\beta(\omega)$ derived from the general formulation (33a).

[1]A. J. Cramond and C. G. Don, "Effects of moisture content on soil impedance," J. Acoust. Soc. Am. **82**, 293–301 (1987).
[2]K. V. Horoshenkov and M. H. A. Mohamed, "Experimental investigation of the effects of water saturation on the acoustic admittance of sandy soils," J. Acoust. Soc. Am. **120**, 1910–1921 (2006).
[3]T. Oshima, Y. Hiraguri, and T. Okuzono, "Distinct effects of moisture and air contents on acoustic properties of sandy soil," J. Acoust. Soc. Am. **138**, EL258–EL263 (2015).
[4]C. Liu and M. Hornikx, "Effect of water content on noise attenuation over vegetated roofs: Results from two field studies," Build. Environ. **146**, 1–11 (2018).
[5]E. Attal, Y. B. de l'Epine, N. Dauchez, and B. Dubus, "Experimental investigation of the effect of moisture on the acoustic properties of lightweight substrates used in green envelopes," Appl. Acoust. **180**, 108108 (2021).
[6]D. L. Johnson, "Theory of frequency dependent acoustics in patchy-saturated porous media," J. Acoust. Soc. Am. **110**, 682–694 (2001).
[7]Y. Mao, "Sound attenuation in a cylindrical tube due to evaporation–condensation," J. Acoust. Soc. Am. **104**, 664–670 (1998).
[8]W. V. Slaton, R. Raspet, and C. J. Hickey, "The effect of the physical properties of the tube wall on the attenuation of sound in evaporating and condensing gas–vapor mixtures," J. Acoust. Soc. Am. **108**, 2120–2124 (2000).
[9]C. Guianvarc'h, M. Bruneau, and R. M. Gavioso, "Acoustics and precondensation phenomena in gas-vapor saturated mixtures," Phys. Rev. E **89**, 023208 (2014).
[10]W. Batson, Y. Agnon, and A. Oron, "Mass variation of a thin liquid film driven by an acoustic wave," Phys. Fluids **27**, 062106 (2015).
[11]R. Venegas and C. Boutin, "Acoustics of sorptive porous materials," Wave Motion **68**, 162–181 (2017).
[12]C. Boutin and R. Venegas, "Acoustics of wet porous media with evaporation/condensation," Phys. Fluids **36**, 103113 (2024).
[13]W. V. Slaton, R. Raspet, C. J. Hickey, and R. A. Hiller, "Theory of inert gas-condensing vapor thermoacoustics: Transport equations," J. Acoust. Soc. Am. **112**, 1423–1430 (2002).
[14]R. Raspet, W. V. Slaton, C. J. Hickey, and R. A. Hiller, "Theory of inert gas-condensing vapor thermoacoustics: Propagation equation," J. Acoust. Soc. Am. **112**, 1414–1422 (2002).
[15]K. Tsuda and Y. Ueda, "Critical temperature of traveling- and standing-wave thermoacoustic engines using a wet regenerator," Appl. Energ. **196**, 62–67 (2017).
[16]R. Yang, A. Meir, and G. Z. Ramon, "A standing-wave, phase-change thermoacoustic engine: Experiments and model projections," Energy **258**, 124665 (2022).
[17]R. Yang, N. Blanc, and G. Z. Ramon, "Environmentally-sound: An acoustic-driven heat pump based on phase change," Energ. Convers. Manage. **232**, 113848 (2021).
[18]G. Ma and P. Sheng, "Acoustic metamaterials: From local resonances to broad horizons," Sci. Adv. **2**, e1501595 (2016).
[19]F. Casadei, T. Delpero, A. Bergamini, P. Ermanni, and M. Ruzzene, "Piezoelectric resonator arrays for tunable acoustic waveguides and metamaterials," J. Appl. Phys. **112**, 064902 (2012).
[20]N. Kherraz, F.-H. Chikh-Bled, R. Sainidou, B. Morvan, and P. Rembert, "Tunable phononic structures using Lamb waves in a piezoceramic plate," Phys. Rev. B **99**, 094302 (2019).
[21]B. Xia, N. Chen, L. Xie, Y. Qin, and D. Yu, "Temperature-controlled tunable acoustic metamaterial with active band gap and negative bulk modulus," Appl. Acoust. **112**, 1–9 (2016).
[22]T.-T. Wang, Y.-F. Wang, Y.-S. Wang, and V. Laude, "Tunable fluid-filled phononic metastrip," Appl. Phys. Lett. **111**, 041906 (2017).
[23]S. Bansal and S. Subramanian, "A microfluidic acoustic metamaterial using electrowetting: Enabling active broadband tunability," Adv. Mater. Tech. **6**, 2100491 (2021).
[24]K. Rasmussen, "Calculation methods for the physical properties of air used in the calibration of microphones," (1997).
[25]I. H. Bell, J. Wronski, S. Quoilin, and V. Lemort, "Pure and pseudo-pure fluid thermophysical property evaluation and the open-source thermophysical property library CoolProp," Ind. Eng. Chem. Res. **53**, 2498–2508 (2014).
[26]D. L. Johnson, J. Koplik, and R. Dashen, "Theory of dynamic permeability and tortuosity in fluid-saturated porous media," J. Fluid Mech. **176**, 379 (1987).
[27]Y. Champoux and J.-F. Allard, "Dynamic tortuosity and bulk modulus in air-saturated porous media," J. Appl. Phys. **70**, 1975–1979 (1991).
[28]D. Lafarge, P. Lemarinier, J. F. Allard, and V. Tarnow, "Dynamic compressibility of air in porous structures at audible frequencies," J. Acoust. Soc. Am. **102**, 1995–2006 (1997).
[29]J. B. Mehl and M. R. Moldover, "Precondensation phenomena in acoustic measurements," J. Chem. Phys. **77**, 455–465 (1982).
[30]S. E. Turner and D. R. Dowling, "Acoustic precondensation phenomena in freons," J. Acoust. Soc. Am. **97**, 1014–1018 (1995).
[31]D. D. Do, *Adsorption analysis: equilibria and kinetics*, Series on chemical engineering No. vol. 2 (Imperial College Press, London, 1998).
[32]C. Guianvarc'h and M. Bruneau, "Acoustic fields in binary gas mixtures: Mutual diffusion effects throughout and beyond the boundary layers," J. Acoust. Soc. Am. **131**, 4252–4262 (2012).
[33]L. D. Landau and E. M. Lifshitz, *Fluid mechanics*, 2nd ed., Course of theoretical physics, Vol. 6 (Pergamon Press, Oxford, England, 1987).
[34]J. V. Hirschfelder, C. Curtiss, and R. Bird, *Molecular Theory Of Gases and Liquids* (Wiley, New York, 1954).
[35]O. Weltsch, A. Offner, D. Liberzon, and G. Z. Ramon, "Adsorption-mediated mass streaming in a standing acoustic wave," Phys. Rev. Lett. **118**, 244301 (2017).
[36]I. E. Dzyaloshinskii, E. M. Lifshitz, and L. P. Pitaevskii, "General theory of van der Waals' forces," Sov. Phys. Usp. **73**, 153–176 (1961).
[37]M. Bruneau, P. Gatignol, P. Lanceleur, and C. Potel, *Exercices d'acoustique: corrigés détaillés, rappels de cours (Acoustics exercises: detailed answers, course reviews)*, Sciences mécaniques, Vol. 2 (Cépaduès-éditions, Toulouse, 2020).
[38]M.-Y. Zhou and P. Sheng, "First-principles calculations of dynamic permeability in porous media," **39**, 12027–12039.
[39]T. G. Zieliński, R. Venegas, C. Perrot, M. Červenka, F. Chevillotte, and K. Attenborough, "Benchmarks for microstructure-based modelling of sound absorbing rigid-frame porous media," J. Sound Vib. **483**, 115441 (2020).
[40]D. L. Johnson, J. Koplik, and L. M. Schwartz, "New pore-size parameter characterizing transport in porous media," Phys. Rev. Lett. **57**, 2564–2567 (1986).
[41]M. Avellaneda and S. Torquato, "Rigorous link between fluid permeability, electrical conductivity, and relaxation times for transport in porous media," Phys. Fluids A-Fluid **3**, 2529–2540 (1991).
[42]L. M. Schwartz, N. Martys, D. P. Bentz, E. J. Garboczi, and S. Torquato, "Cross-property relations and permeability estima-

tion in model porous media," Phys. Rev. E **48**, 4584–4591 (1993).
[43]M. R. Stinson, "The propagation of plane sound waves in narrow and wide circular tubes, and generalization to uniform tubes of arbitrary cross-sectional shape," J. Acoust. Soc. Am. **89**, 550–558 (1991).